

000 001 002 003 004 005 006 007 008 009 010 011 012 013 014 015 016 017 018 019 020 021 022 023 024 025 026 027 028 029 030 031 032 033 034 035 036 037 038 039 040 041 042 043 044 045 046 047 048 049 050 051 052 053 DISTRIBUTIONAL MACHINE UNLEARNING VIA SELECTIVE DATA REMOVAL

Anonymous authors

Paper under double-blind review

ABSTRACT

Machine learning systems increasingly face requirements to remove entire domains of information—such as toxic language or biases—rather than individual user data. This task presents a dilemma: full removal of the unwanted domain data is computationally expensive, while random partial removal is statistically inefficient. We find that a domain’s statistical influence is often concentrated in a small subset of its data samples, suggesting a path between ineffective partial removal and unnecessary complete removal. We formalize this as *distributional unlearning*: a framework to select a small subset that balances forgetting an unwanted distribution while preserving a desired one. Using Kullback-Leibler divergence constraints, we derive the exact removal-preservation Pareto frontier [for Gaussian distributions](#) and prove that models trained on the edited data achieve corresponding log-loss bounds. We propose a distance-based selection algorithm and show it is quadratically more sample-efficient than random removal in the challenging low-divergence regime. Experiments across synthetic, text, and image datasets (Jigsaw, CIFAR-10, SMS spam) show our method requires 15–82% less deletion than full removal for strong unlearning effects, e.g., halving initial forget set accuracy. Ultimately, by showing a small forget set often suffices, our framework lays the foundations for more scalable and rigorous subpopulation unlearning.

1 INTRODUCTION

As machine learning models persist in production, the data on which they were trained often becomes legally or ethically objectionable, requiring deletion. The nature of these requests is now scaling beyond individual user data towards erasing entire subpopulations, which can represent unwanted domains, concepts, or any data-defined construct, e.g., harmful biases or toxic language (Kurmanji et al., 2024). This new scale of unlearning presents a dilemma. On one hand, removing the full set of domain data involves a prohibitive cost, since the computational cost of efficient removal methods typically scales with the size of the forget set (Guo et al., 2020). This challenge is highlighted in efforts to unlearn creative works like the Harry Potter book series (Eldan & Russinovich, 2023), where the sheer size of the identified text and the trained model make the subsequent unlearning action computationally expensive. On the other hand, removing a random small subset can be statistically inefficient because the statistical footprint of the domain persists. For instance, large language models can still verbatim reproduce training sequences even if the specific source text is removed (Liu et al., 2025), due to overlapping context with the remaining data. This dilemma, between the expensive cost of full removal and the ineffectiveness of naive partial removal, leaves a methodological gap for a more targeted and efficient approach to domain unlearning.

To address this methodological gap, we start with a key observation: a domain’s statistical influence is often concentrated in a small, high-impact subset of its samples. This suggests an optimal strategy exists between the two extremes: a targeted removal of only this impactful subset, which can be both computationally efficient and statistically effective. To formalize this, we model domains as unknown probability distributions, a well-precedented abstraction in both statistical learning (Shalev-Shwartz & Ben-David, 2014) and natural language processing (Blei et al., 2003; Srivastava & Sutton, 2017). This statistical framing allows us to pose a precise research question: *what is the minimal set of data points to remove to make the data distribution far from an unwanted domain, yet simultaneously close to a retained one?* We introduce *distributional unlearning*, an information-theoretic framework that quantitatively addresses this question. [This data-centric, statistical framing is complementary to the rich literature on what we term *sample-level* unlearning: methods that efficiently approximate retraining without a pre-defined set of individual records.](#) While prior work on sample-level methods, based on influence functions (Guo et al., 2020) or data

sharding (Bourtoule et al., 2021), have made important progress on the *computational* problem, they do not address the *statistical* question of which samples should constitute that set for maximal impact. Similarly, while class-level unlearning (Tarun et al., 2023; Kodge et al., 2024) and concept erasure (Ravfogel et al., 2020; Belrose et al., 2023) methods also operate on certain domains, they either act on a model’s internal representations—making the changes potentially reversible—or lack a formal method for finding a small subset to remove. This leaves our foundational question unanswered: which samples to remove in the first place?

Contributions. We summarize our contributions in tackling the above question as follows:

- *Framework:* We formalize distributional unlearning, a data-centric framework that uses Kullback-Leibler divergence constraints to balance removal and preservation guarantees.
- *Pareto frontier & downstream guarantees:* We derive the closed-form Pareto frontier of achievable removal-preservation levels for exponential families. We further prove our framework provides log-loss shift guarantees for downstream models.
- *Algorithm & sample efficiency:* We study the sample complexity of distributional unlearning with both random and selective removal mechanisms. We propose a distance-based selection algorithm and prove that it achieves a quadratic improvement in sample efficiency over random removal in low-divergence Gaussian regimes.
- *Empirical validation:* We validate our framework on synthetic, text, and image data (Jigsaw, CIFAR-10, SMS spam). While our synthetic analysis suggests high potential data efficiency gains up to 82%, real-world data complexity reduces these to a still-significant 15–50% in deletion budget savings. We show these data savings to hold in combination with various downstream sample-level unlearning methods.

1.1 RELATED WORK

Sample-level unlearning. Sample-level unlearning has made impressive strides in fast model updates and formal deletion guarantees (Neel et al., 2021; Zhang et al., 2024a; Chien et al., 2024; Allouah et al., 2025; Koloskova et al., 2025). Izzo et al. (2021) use influence-function updates to approximate the effect of deleting a single point without full retraining; Guo et al. (2020) provide certified bounds on how close the post-deletion model is to a scratch-retrained one; Bourtoule et al. (2021) employ data sharding to efficiently erase small batches. However, this class of methods does not address which or how many samples must be removed to eliminate a domain’s overall statistical footprint. Our work complements these techniques by asking not just how to update a model once samples are flagged, but which samples to flag in the first place, and in what quantity.

Concept erasure. Concept erasure methods tackle unwanted attributes in learned features. INLP (Ravfogel et al., 2020) repeatedly projects out directions predictive of a protected attribute; counterfactual augmentation (Kaushik et al., 2020) synthesizes targeted data to sever causal links; adversarial training (Elazar & Goldberg, 2018) trains encoders to remove specific signals. These operate post-hoc on a fixed model’s representations—ideal for fairness use-cases such as removing gender—but they rely on white-box access and tailor to one model at a time. Where concept erasure edits model representations, we edit the data, guaranteeing forgetting for downstream models.

Coresets & domain adaptation. Domain adaptation theory (Ben-David et al., 2010) seeks to minimize the impact of divergence between domains; we flip this paradigm by intentionally increasing divergence from an unwanted source while controlling proximity to a desired one. Similarly, our work inverts the goal of coresets, which approximate a single distribution for efficient training (Mirza-soleiman et al., 2020; Gentile et al., 2024). Coreset methods are designed for a one-distribution problem, whereas we select samples from an unwanted distribution based on their relationship to a separate, retained distribution. This two-distribution approach is critical; our experiments show that a coreset-based baseline is inefficient for unlearning because it ignores the retain data.

2 DISTRIBUTIONAL UNLEARNING: DEFINITION AND IMPLICATIONS

The predominant paradigm in machine unlearning, which we call sample-level unlearning, addresses the computational challenge of fully removing a known finite set of data points. This work addresses a *complementary* scenario, which we call distributional unlearning, where the goal is to erase the statistical influence of a subpopulation. In this section, we formalize this task, establish its fundamental trade-offs, and prove its consequences for downstream predictors.

108 **Problem Statement.** To make the abstract concept of the unwanted domain tractable, we first model
 109 it as an underlying probability distribution p_1 . This abstraction, common in statistical machine
 110 learning, allows us to set a mathematical objective: to construct a new data distribution p that is
 111 statistically distant from p_1 yet remains close to a retained distribution p_2 . In practice, these true
 112 distributions are unknown. We instead work with finite sets of samples: $S_1 = \{x_i^{(1)}\}_{i=1}^{n_1}$ drawn
 113 i.i.d. from unwanted distribution p_1 , and $S_2 = \{x_j^{(2)}\}_{j=1}^{n_2}$ from retained distribution p_2 . **Crucially,**
 114 **we assume these sets are obtained via some upstream process, such as keyword filtering (as in our**
 115 **Jigsaw experiments), the output of a pre-trained classifier, or human annotation.** Our contribution is
 116 to solve the subsequent statistical problem: given these identified samples, which subset should be
 117 removed to most efficiently achieve our objective defined at the distribution level?

118 To formalize our objective, we choose Kullback-Leibler (KL) divergence because it enables con-
 119 trol over the expected log-loss of downstream models, hence connecting data-level edits to pre-
 120 dictive outcomes. We recall for two absolutely-continuous distributions q, p on data space \mathcal{X} that
 121 $\text{KL}(q\|p) := \int_{\mathcal{X}} q(x) \log \frac{q(x)}{p(x)} dx$.

122 **Definition 1** ((α, ε)-Distributional Unlearning). *For tolerances $\alpha, \varepsilon > 0$, a distribution $p \in \mathcal{P}$ satis-
 123 fies (α, ε) -distributional unlearning with respect to (p_1, p_2) if:*

$$124 \text{KL}(p_1 \| p) \geq \alpha \quad (\text{removal}), \quad \text{KL}(p_2 \| p) \leq \varepsilon \quad (\text{preservation}). \quad (1)$$

125 The first inequality forces the edited data to be information-theoretically distant from the popula-
 126 tion we wish to forget. The second inequality upper bounds collateral damage to the population
 127 we preserve. **While we focus on KL divergence for its analytical tractability and its direct control**
 128 **of expected log-loss, we note that different tasks may favor different divergences, and our frame-**
 129 **work can in principle accommodate alternative or task-weighted notions of discrepancy.** In the
 130 remainder of this section, we analyze the properties of this definition at the population level, captur-
 131 ing the fundamental trade-offs and downstream learning-theoretic guarantees. In Section 3, we turn
 132 to the practical finite-sample setting and provide high-probability guarantees for specific removal
 133 algorithms. Throughout, we defer all proofs to Appendix A.

134 **Removal-Preservation Trade-off.** The pair (α, ε) captures a trade-off: how far we can move
 135 from p_1 while remaining close to p_2 . To understand which (α, ε) pairs are jointly achievable, we
 136 characterize the feasible region and its boundary. Formally, the *Pareto frontier* $\text{PF}(p_1, p_2; \mathcal{P})$ con-
 137 sists of those pairs (α, ε) for which no strictly better trade-off exists: there is no $p' \in \mathcal{P}$ satisfying
 138 $\text{KL}(p_1 \| p') \geq \alpha'$ and $\text{KL}(p_2 \| p') \leq \varepsilon'$ with $\alpha' > \alpha$ and $\varepsilon' < \varepsilon$. That is, every point on the frontier
 139 is optimal in the sense that one objective cannot be improved without worsening the other. To build
 140 intuition, we first derive this frontier for the analytically tractable case of Gaussian distributions.

141 **Proposition 1** (Pareto Frontier). *Let p_1, p_2 be two distributions in \mathcal{P} , the class of Gaussian distri-
 142 butions with shared positive covariance. The Pareto frontier of (α, ε) values achievable in \mathcal{P} is:*

$$143 \text{PF}(p_1, p_2; \mathcal{P}) = \left\{ \left(\alpha, \left(\sqrt{\alpha} - \sqrt{\text{KL}(p_1 \| p_2)} \right)^2 \right) : \alpha \geq \text{KL}(p_1 \| p_2) \right\}.$$

144 This frontier quantifies a natural, fundamental cost of distributional unlearning: a minimal preser-
 145 vation loss is incurred for any given removal level, a trade-off governed by the initial divergence
 146 $\text{KL}(p_1 \| p_2)$. The result also highlights the suboptimality of a common default: keeping only the
 147 retained data p_2 . While this strategy achieves perfect preservation, the frontier shows it is possible
 148 to attain a significantly higher level of removal by accepting a potentially small preservation loss.
 149 While shown here for Gaussians for simplicity, this trade-off holds more generally for regular expo-
 150 nential families (Appendix A, Theorem 4) and is validated by our synthetic experiments (Fig. 1).

151 **Downstream Performance.** We now connect our data-level objective to predictive performance in
 152 supervised learning. Consider a predictor $h : \mathcal{X} \rightarrow \Delta(\mathcal{Y})$, where \mathcal{X} is the input space and $\Delta(\mathcal{Y})$
 153 the probability simplex over label space \mathcal{Y} , trained on a distribution p over $\mathcal{X} \times \mathcal{Y}$ that satisfies
 154 (α, ε) -distributional unlearning with respect to (p_1, p_2) . We study how h performs under the true
 155 data-generating distributions p_1 and p_2 .

156 Let $\ell(y, q) := -\log q(y)$, for $y \in \mathcal{Y}, q \in \Delta(\mathcal{Y})$, denote the log-loss. Define the expected loss under
 157 p as $\mathcal{L}(h; p) := \mathbb{E}_{(x, y) \sim p}[\ell(y, h(x))]$. Then, for any class of distributions \mathcal{P} , we have:

158 **Proposition 2.** *Let h minimize $\mathcal{L}(h; p)$, and let h_1, h_2 be optimal predictors under $p_1, p_2 \in \mathcal{P}$,
 159 respectively. If p satisfies (α, ε) -distributional unlearning with respect to (p_1, p_2) , then:*

$$160 \mathcal{L}(h; p_1) - \mathcal{L}(h_1; p_1) \geq \alpha - \delta_1, \quad \mathcal{L}(h; p_2) - \mathcal{L}(h_2; p_2) \leq \varepsilon - \delta_2, \quad (2)$$

| 162 | 163 | 164 | 165 | Removal Method | Sample Complexity | |
|-----|-----|-----|-----|--------------------|--------------------------------|--------------------------------|
| | | | | 166 | Removal | Preservation |
| 167 | 168 | 169 | 170 | Random (Prop. 3) | $n_1 (1 - \sqrt{1 - \alpha})$ | $n_1 (1 - \sqrt{\varepsilon})$ |
| 171 | 172 | 173 | 174 | Selective (Thm. 1) | $n_1 (1 - (1 - \alpha)^{1/4})$ | $n_1 (1 - \varepsilon^{1/4})$ |

Table 1: Summary of *simplified* sample complexity bounds, showing the number of p_1 samples (out of $n_1 \geq 1$) to remove to achieve (α, ε) -distributional unlearning with high probability. We assume n_2 is large, $\text{KL}(p_1 \| p_2)$ is small, and $\frac{n_2}{n_1}$ is constant; see Corollary 10 for details. The key insight is the quadratic improvement in sample efficiency of selective removal over random in this regime.

where $\delta_1 := \text{KL}(p_{1,X} \| p_X)$, $\delta_2 := \text{KL}(p_{2,X} \| p_X)$ denote the marginal KL divergence over inputs.

These bounds show that distributional unlearning guarantees increased loss under the forgotten distribution and bounded degradation under the preserved one. In this sense, our framework provides meaningful control over downstream predictive behavior. Regarding the extra marginal KL term in the first inequality, which quantifies divergence on input distributions, the data-processing inequality gives $\text{KL}(p_{1,X} \| p_X) \leq \text{KL}(p_1 \| p)$, hence this extra term is always bounded by the same α we already control. A similar term appears in the second inequality, but can only improve the preservation bound. Finally, these bounds provide a practical rule for calibrating the (α, ε) parameters. For instance, if a practitioner decides they can tolerate at most a 0.1 nat increase in log-loss on the retained test set, they can set their preservation budget to $\varepsilon = 0.1$. Then, the Pareto frontier (Prop. 1) indicates the maximum achievable removal for this budget, in the Gaussian case. In a scenario where the initial distributions have divergence $\text{KL}(p_1 \| p_2) = 2$, this choice of ε corresponds to the removal target of $\alpha = 3$. These values match our findings in controlled experiments (Fig. 2, 2nd column).

3 ALGORITHMS AND SAMPLE COMPLEXITY

The previous section defined our framework at the population level. We now turn to the practical finite-sample setting, where we must achieve (α, ε) -distributional unlearning using only the drawn data samples introduced in Section 2. To build an analytical understanding of the finite-sample behavior, we analyze the problem in an idealized but foundational setting: univariate Gaussian distributions with known variance. This tractable setting allows us to derive closed-form sample complexity bounds, providing crucial intuition about the relative efficiency of different removal strategies. We then validate that these insights generalize empirically to more complex settings in Section 4.

In the following, we introduce and analyze two deletion strategies: a random baseline and a selective, distance-based method. We focus on the class of distributions $\mathcal{P} := \{\mathcal{N}(\mu, \sigma^2) : \mu \in \mathbb{R}\}$, with known $\sigma > 0$. Given n_1 i.i.d. samples from the unwanted distribution $p_1 \in \mathcal{P}$ and n_2 from the retained distribution $p_2 \in \mathcal{P}$, and a deletion budget $0 \leq f \leq n_1$, we derive high-probability bounds on the resulting (α, ε) -distributional unlearning guarantees. We defer all proofs to Appendix A.

3.1 RANDOM REMOVAL

We begin with a baseline deletion strategy that treats every sample equally, deleting f points chosen uniformly at random from the n_1 samples of p_1 . The formal procedure is as follows:

Algorithm (Random Removal).

1. Randomly select f out of the n_1 samples of p_1 without replacement.
2. Remove those f samples.
3. Re-fit $\mathcal{N}(\hat{\mu}, \sigma^2)$ by MLE (maximum likelihood estimation) on the remaining data.

The following theorem provides a finite-sample guarantee for achieving (α, ε) -distributional unlearning using random removal with a deletion budget f .

Proposition 3 (Random Removal). *Let $p_1, p_2 \in \mathcal{P}$ and $\delta \in (0, 1)$. We observe n_1 samples from p_1 and n_2 samples from p_2 , and randomly remove f samples from p_1 before fitting. With probability $1 - \delta$, the resulting MLE distribution satisfies (α, ε) -distributional unlearning with:*

$$\alpha \geq \left(\frac{1}{2} - 3 \left(\frac{n_1 - f}{n_2} \right)^2 \right) \text{KL}(p_1 \| p_2) - \frac{3 \ln(4/\delta)}{2n_2} \left(1 + \frac{n_1 - f}{n_2} \right),$$

$$\varepsilon \leq 3 \left(\frac{n_1 - f}{n_2} \right)^2 \text{KL}(p_1 \| p_2) + \frac{3 \ln(4/\delta)}{n_2} \left(1 + \frac{n_1 - f}{n_2} \right).$$

This result shows that the effectiveness of random removal is driven by the ratio of remaining unwanted samples to retained samples $\frac{n_1-f}{n_2}$. An interesting aspect of these bounds is the quadratic dependence on this ratio, which indicates diminishing returns: each subsequent random deletion provides progressively less of an unlearning effect. This quadratic relationship stems from the concentration of the empirical mean, whose variance scales inversely with the sample size. While conceptually simple, this method’s inefficiency arises because it treats all samples equally, failing to prioritize those that contribute most to the unwanted statistical patterns.

3.2 SELECTIVE REMOVAL

We hypothesize that a more effective strategy than random removal should prioritize which samples to delete, using p_2 as reference. Since our goal is to shift the dataset’s empirical mean away from the unwanted center μ_1 and towards the retained center μ_2 , the most impactful samples to remove are those from p_1 that are furthest from μ_2 . This intuition leads to our proposed selective removal strategy, which uses the empirical mean of the retained data $\hat{\mu}_2$ as a reference point for selection.

Algorithm (Selective Removal).

1. Compute the mean $\hat{\mu}_2$ of the n_2 samples from p_2 .
2. For each of the n_1 samples x_i from p_1 , compute the score $s_i = |x_i - \hat{\mu}_2|$.
3. Delete the f samples with the largest scores s_i .
4. Re-fit $\mathcal{N}(\hat{\mu}, \sigma^2)$ by MLE on the remaining data.

The following theorem provides a finite-sample guarantee for achieving (α, ε) -distributional unlearning using selective removal with a deletion budget f .

Theorem 1 (Selective Removal). *Let $p_1, p_2 \in \mathcal{P}$ and $\delta \in (0, 1)$. Let f samples from p_1 be removed according to Selective Removal. With probability $1 - \delta$, the resulting estimate satisfies (α, ε) -distributional unlearning with:*

$$\alpha \geq \frac{1}{2} \text{KL}(p_1 \parallel p_2) - \frac{1}{2} \left(\frac{n_1 - f}{n_2} \right)^2 g^{-1} \left(1 - \frac{f}{n_1} + \sqrt{\frac{\ln(4/\delta)}{2n_1}}; \text{KL}(p_1 \parallel p_2) \right)^2 - \frac{\ln(4/\delta)}{n_2},$$

$$\varepsilon \leq \left(\frac{n_1 - f}{n_2} \right)^2 g^{-1} \left(1 - \frac{f}{n_1} + \sqrt{\frac{\ln(4/\delta)}{2n_1}}; \text{KL}(p_1 \parallel p_2) \right)^2 + \frac{2\ln(4/\delta)}{n_2},$$

where $g(u; \kappa) := \Phi(u - \sqrt{2\kappa}) + \Phi(u + \sqrt{2\kappa}) - 1$, for $u, \kappa > 0$, and Φ is the standard normal CDF.

While the above expression is more complex than that of Prop. 3, it reveals a significant improvement in efficiency, materialized in the term involving the inverse CDF $g^{-1}(\cdot; \kappa)$. Intuitively, this term represents a quantile of a folded normal distribution, shifted by $\kappa = \text{KL}(p_1 \parallel p_2)$, and arises because we are truncating the distribution of scores by removing those in the tail. Specifically, this term strictly amplifies the quadratic decrease in f , which was the best we could previously obtain with random removal. This amplification is greatest when the distributions are close (the low-divergence regime), as the “outlier” samples are more distinct and their removal provides a greater and more targeted shift in the empirical mean. As we summarize in Table 1 and derive formally in Corollary 10 (Appendix A), this improved leverage translates directly into a quadratic improvement in sample efficiency over the random baseline in low-divergence regimes. This theoretical advantage is a core finding of our work and is empirically validated in our experiments (Fig. 2).

4 EMPIRICAL VALIDATION

We now empirically evaluate our distributional unlearning framework across several case studies, moving from synthetic to more complex real-world data. These experiments are designed to validate the qualitative trends predicted by our theory—notably, the superior sample efficiency of selective removal—rather than to directly apply Theorem 1 and Proposition 3, which assume Gaussianity. To this end, we operationalize abstract domains using well-defined proxies, e.g., keyword-based subsets, image classes. This allows for a reproducible evaluation of our selection algorithms, while acknowledging that the upstream task of identifying such domains in the wild is a separate challenge.

Our validation begins with synthetic Gaussians to directly verify our theoretical predictions in a controlled environment. [We then move to high-dimensional real-world data, starting with the case](#)

| Domain | Separability | Target on p_1 | Random | Selective | Savings |
|-----------------------|--------------|---------------------|--------|-----------|-------------|
| Gaussians | Low | $\text{KL}(p_1\ p)$ | 65 | 18 | 82 % |
| Gaussians | High | $\text{KL}(p_1\ p)$ | 65 | 50 | 50 % |
| Jigsaw toxic comments | Low | Recall | 100 | 85 | 15 % |
| SMS Spam | Medium | Recall | 90 | 75 | 25 % |
| CIFAR-10 | High | Accuracy | 80 | 50 | 50 % |

Table 2: Deletion budget (%) needed to reach half of the initial value of the removal metric (no deletion) on each dataset. “Selective”=best-performing selective removal score; “Saving”=relative size reduction versus full removal, i.e. retrain on p_2 samples only. Gaussians (low) and (high) are the scenarios of the top leftmost and rightmost plots of Fig. 2, respectively. “Separability”=summarizes how distinguishable the domains are; the observed savings follow this difficulty.

of well-separated distributions (CIFAR-10), showing our framework generalizes standard class unlearning. We then test our framework in the more challenging scenario of intertwined distributions (Jigsaw toxic comments), where the unwanted domain is semantically linked to the main task. Finally, we demonstrate the broad applicability of our data-centric approach by using it as an efficiency-boosting front-end for existing sample-level unlearning algorithms. We defer results on an additional text dataset (SMS Spam) and full experimental details to Appendix B.

Results overview. We summarize our main empirical findings in Table 2. Our synthetic experiments directly validate our theory, showing data savings of up to 82% in the low-divergence Gaussian regime, where our analysis predicts the greatest advantage. Crucially, this insight generalizes to high-dimensional non-Gaussian text and image data, where selective methods still provide significant 15–50% data savings. As expected, the magnitude of these gains is more modest than in the idealized theoretical setting, reflecting the increased complexity of real-world distributions. Across all experiments, these removal gains are achieved with negligible impact on performance on the retained domains, confirming the downstream performance guarantees predicted by Proposition 2. In particular, the intertwined distribution case study on Jigsaw confirms that simply deleting all p_1 is suboptimal, as discussed after Proposition 1. Finally, we show in Table 5 that our selection methods combine effectively with various sample-level unlearning methods, not just retraining from scratch.

4.1 SYNTHETIC GAUSSIANS: PARETO FRONTIER AND SAMPLE EFFICIENCY

We first validate our theoretical framework in a controlled setting, designed to directly verify the analytical predictions made in Sections 2 and 3: the Pareto frontier shape and the superior sample efficiency of selective removal. We set $p_1 = \mathcal{N}(0, 1)$ and $p_2 = \mathcal{N}(\mu, 1)$ for varying $\mu \in \{0.5, 2.5, 5\}$, which allows controlling the initial divergence $\text{KL}(p_1\|p_2)$, i.e., intertwinement level. For each configuration, we draw $n_1 = n_2 = 1000$ samples from p_1 and p_2 , respectively. We implement the two mechanisms from Section 3: *random* and *selective* removal. After deleting f samples, we re-fit a Gaussian $p = \mathcal{N}(\hat{\mu}, 1)$ on the retained p_1 and p_2 samples. We then compute forward KL divergences $\alpha = \text{KL}(p_1\|p)$ and $\varepsilon = \text{KL}(p_2\|p)$ to quantify forgetting and preservation, respectively.

Pareto frontier. Figure 1 confirms that the empirical (α, ε) trade-off closely matches the theoretical Pareto frontier derived in Proposition 1. To plot feasible empirical trade-offs, we set $p = \mathcal{N}(\mu, 1)$ and vary $\mu \in \mathbb{R}$, while $p_1 = \mathcal{N}(0, 1)$ and $p_2 = \mathcal{N}(2, 1)$ so that $\text{KL}(p_1\|p_2) = 2$. The latter quantity is the threshold predicted by the theory, and validated by Figure 1. Indeed, feasible trade-offs whose removal divergence α is below this threshold are pareto-suboptimal. They are dominated by the trade-off $(\alpha = \text{KL}(p_1\|p_2), \varepsilon = 0)$, which can be achieved with the choice of distribution $p = p_2$.

Sample efficiency. We next compare the sample efficiency of the two removal strategies analyzed in Section 3. In Figure 2, we plot removal α as a function of the number of p_1 samples removed. Selective removal reaches higher forgetting levels with fewer deletions than random removal, especially in the low-divergence regime ($\mu_2 = 0.5$, top left plot). For example, to reach 0.06 nats of removal divergence, i.e., half of that obtained by removing all samples, selective removal requires $5 \times$ less samples than random removal, i.e., $10 \times$ reduction in size from full removal. Analogous trends hold for preservation (bottom left plot): selective removal more effectively preserves the reference distribution p_2 throughout. The remaining plots show similar

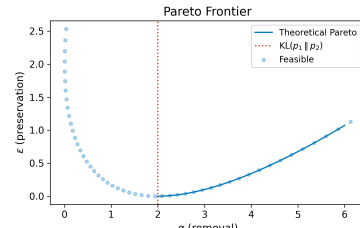


Figure 1: **Synthetic Gaussians.** The empirical frontier aligns with the theoretical prediction.

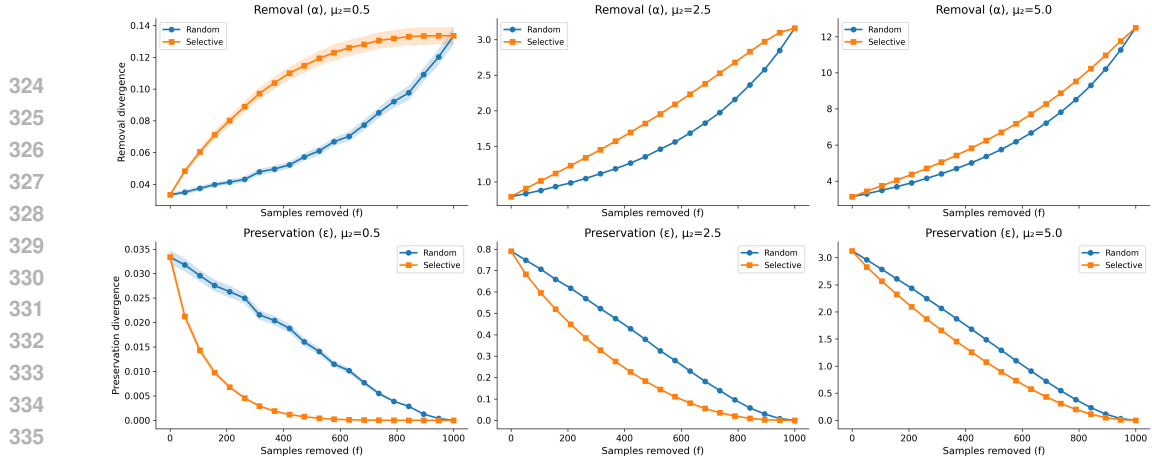


Figure 2: **Synthetic Gaussians.** Selective removal consistently requires fewer deletions, especially when $\text{KL}(p_1\|p_2)$ is small (left), for the same removal and preservation target as random removal. In high-divergence regimes (right), the gap between methods shrinks, as predicted by the theory.

trends when increasing the divergence $\text{KL}(p_1\|p_2)$ by increasing μ_2 . As in theory, selective removal offers the greatest savings when p_1 and p_2 are close and diminishes as the distributions diverge.

4.2 CASE STUDIES IN REAL-WORLD DATA

Having validated our theoretical predictions in a controlled setting, we now test our framework’s applicability on high-dimensional non-Gaussian data. We present two case studies representing distinct unlearning scenarios. We first analyze the CIFAR-10 dataset (Krizhevsky et al., 2014) to test our framework on well-separated distributions, showing it generalizes standard class unlearning. We then turn to the Jigsaw toxic comments dataset¹ for the more challenging scenario of intertwined distributions, where the unwanted domain is semantically linked to the main task.

Removal methods. Across both case studies, we evaluate several scoring heuristics designed to rank samples in the unwanted distribution p_1 for selective removal. These heuristics are high-dimensional analogues inspired by the principles developed in our theoretical analysis. The choice of distance metric is adapted to the data modality: for the sparse, high-dimensional TF-IDF text embeddings, we use Cosine distance; for the dense CNN image features, where feature covariance is meaningful, we use Mahalanobis distance². Our main selective removal strategies are: (1) distance to retained (COS-MU2 / MAHA-MU2): this heuristic is a direct analogue of the distance-based method formally analyzed in Section 3. It scores samples based only on their distance to the mean of the retained distribution p_2 , in cosine and Mahalanobis distance respectively; (2) likelihood-ratio (LR-COS / LR-MAHA): this is an extension that scores samples based on a margin between their distance to the p_2 mean versus their distance to the p_1 mean, aiming to remove samples that are both distinguishable from p_2 and representative of p_1 , in cosine and Mahalanobis distance respectively; (3) Local Density Ratio (KNN-RATIO): This heuristic estimates the local density ratio around a sample using its k -nearest neighbors ($k = 10$). It aims to remove samples that are much more “typical” of the unwanted distribution p_1 than the retained distribution p_2 in their immediate feature neighborhood; (4) Feature Norm (TFIDF-NORM): This simpler baseline scores samples based on the ℓ_2 -norm of their feature vector. It serves as a proxy for a sample’s “informativeness” or extremity in the feature space. We further discuss their computational complexity in Remark 12. **While our selection rules follow directly from the Gaussian analysis, we note that real-world distributions can be multimodal, in which case more expressive criteria, e.g., incorporating local density or cluster structure, may further improve performance.**

Our scoring functions compute similarity between forget and retain samples using finite-sample estimates, e.g., empirical means or embeddings. When only a small or proxy retain subset is available, as may occur in large-scale settings, these estimates become noisier but still supply a meaningful signal, and the distributional unlearning framework applies without modification. Extending these

¹<https://www.kaggle.com/competitions/jigsaw-toxic-comment-classification-challenge>

²The Mahalanobis distance of vector x to probability distribution p , of mean μ and covariance Σ , is: $d(x, p) := \sqrt{(x - \mu)^\top \Sigma^{-1} (x - \mu)}$. We estimate μ and Σ empirically on the retained distribution p_2 .

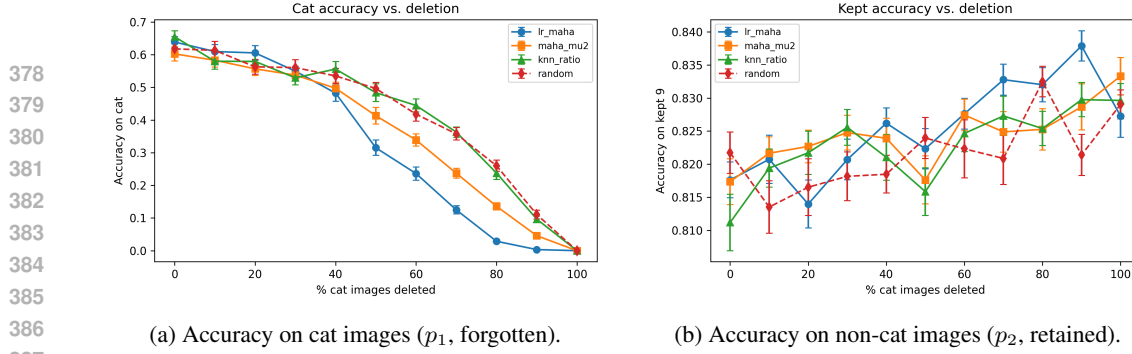


Figure 3: **CIFAR-10 images.** Removing cat images suppresses accuracy on that class (left) while leaving accuracy on the retained nine classes essentially unchanged (right, <0.03 variation). No substantial removal is observed until 50% deletion, before selective removal strategies LR-MAHA and MAHA-MU2 outperform random removal. Error bars: ± 1 standard error over thirty seeds.

ideas to settings such as large language models, where the retain distribution may be approximated by a general-capabilities corpus, is a natural direction for future work.

Remark 2 (Selection Budget Choice). *In practical deployments, the deletion budget can be chosen in two complementary ways. First, budget may be constrained by the computational cost of a downstream sample-level unlearning method, in which case one simply targets the largest forget-set size that satisfies this constraint. Second, one may inspect the cumulative distribution of selection scores and choose the smallest subset of samples that accounts for a desired fraction of the total influence (e.g., 80%), analogous to coverage thresholds used in data pruning.*

4.2.1 CIFAR-10: VALIDATION ON WELL-SEPARATED DISTRIBUTIONS

We first validate our framework on well-separated distributions using the CIFAR-10 dataset, treating the ‘cat’ class as the unwanted domain to simulate common class-level unlearning tasks. This allows us to test a key hypothesis: that even within a single, well-defined class, the statistical influence distinguishing it from other classes is not uniformly distributed among its members. To test this, we rank all ‘cat’ images based on distance scores computed in the feature space of a CNN model, aiming to find the subset whose removal most efficiently erases the class’s statistical footprint. We delete the top score-ranked samples for each deletion budget, re-train a convolutional neural network for ten epochs, and report accuracy on the cat test set and accuracy on the other nine classes test set.

Findings. The results in Figure 3 confirm our hypothesis. The superior sample efficiency of selective methods shows that even within a single class, statistical influence is concentrated. For instance, the LR-MAHA strategy halves the initial accuracy on the ‘cat’ class by deleting only 50% of the images, making it 1.6× more data-efficient than random removal. By removing the most statistically distinct cats first, our data-centric approach accelerates the unlearning process while leaving performance on the other nine classes stable (Fig. 3b). This demonstrates our framework’s value in class unlearning scenarios, offering a more targeted and efficient alternative to naive or complete removals.

4.2.2 JIGSAW TOXIC COMMENTS: INTERTWINED DISTRIBUTION CHALLENGE

We now test our framework on intertwined distributions using the Jigsaw toxic comments dataset. Here, the unwanted domain—comments containing specific profanities (8.6% of the corpus, chosen keywords in Appendix B)—contains strong predictive signals for the main task of identifying toxicity in the retained, non-profanite comments. This creates a high-stakes trade-off where simply removing the entire unwanted p_1 samples harms utility, a fact demonstrated by the sharp drop in performance at full deletion in our experiments (Figure 4b). The objective is therefore to remove the influence of explicit profanity while preserving the shared predictive features.

Findings. Our results validate the need for a targeted strategy in this setting. Figure 4a shows that recall on profane comments remains high until large deletion budgets are reached, confirming the hardness of the task and suggesting that naively removing random profane comments—which may be statistically similar to non-profanite text—is ineffective. A significant unlearning effect is only achieved by selective strategies like LR-COS, which prioritize removing outlier, distinguishable comments. For example, to reduce recall on the profane set to 0.70, the LR-COS strategy achieves this same effect by deleting 80%, a 15% reduction in the required deletion budget compared to random removal, while relatively maintaining performance on the retained set unlike complete removal.

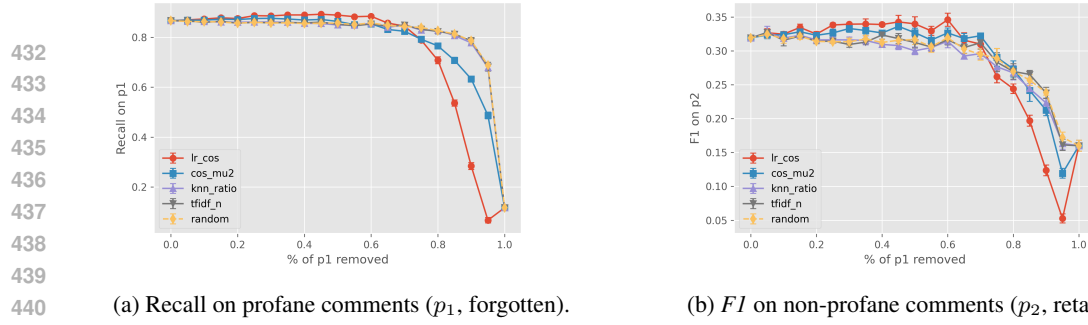
(a) Recall on profane comments (p_1 , forgotten). (b) F_1 on non-profanic comments (p_2 , retained).

Figure 4: **Jigsaw Toxic Comments.** Impact of removing profane comments on Jigsaw Toxic. *Left:* recall on the to-be-forgotten set p_1 ; *right:* F_1 on the retained set p_2 . Utility is almost unchanged up to 60% deletion; marked forgetting appears only around 80% deletion, with LR-COS showing the steepest drop. Error bars: ± 1 standard error over five randomness seeds.

4.3 SYNERGY WITH SAMPLE-LEVEL UNLEARNING

A key application of our data-centric framework is to serve as an efficiency-boosting front-end for various sample-level unlearning algorithms, as their computational cost typically scales with the size of the flagged forget set (e.g., fewer gradients on forget data, see Remark 11). First, on Gaussian data, we pair our selection method with full retraining and a standard influence function-based approximation using the log-likelihood Hessian. Second, on our more complex CIFAR-10 class unlearning task, we pair with recent methods, including finetuning and advanced, gradient-based techniques like NegGrad+ (Kurmanji et al., 2024) and SalUn (Fan et al., 2024) (App. B.2.2). The results, summarized in Table 5, show a consistent and significant improvement in sample efficiency. This advantage is most pronounced in the synthetic, low-divergence setting where our method is up to 5× more sample-efficient, and it qualitatively generalizes to the CIFAR-10 task, where our method uses a deletion budget up to 2× smaller than full removal, while achieving a strong unlearning effect, i.e., 20% test accuracy on forget data, with original $\approx 86\%$ test accuracy on the retained data. Savings vary following the quality of sample-level unlearning, which is poor for naive finetuning, and much more interesting for SalUn, which approximates the retraining standard well.

We compare against a centroid-based coresset baseline that removes the samples most representative of p_1 (those closest to its mean); we also evaluated k -center greedy (recalled in App. B.2.1) which performs near-identically. This strategy performs poorly because, in low-divergence settings, it removes exactly the samples that are least distinguishable from p_2 —the opposite of our selective method. While more sophisticated coresset methods exist, they are designed to preserve the properties of a single distribution. Our dual-distribution objective—to maximize divergence from p_1 while minimizing divergence with respect to p_2 —is fundamentally different. **We hypothesize that any method optimizing for within-distribution representativeness will underperform our cross-distributional approach, and leave a deeper adaptation of coresset methods to future work.** Indeed, our experiments in Section B.4 with two strong gradient-based coressets (CRAIG (Mirzasoleiman et al., 2020), GradMatch (Killamsetty et al., 2021)) illustrate this limitation empirically, as both outperform random deletion yet fall substantially short of our distributional selection under matched budgets. Similarly, recent pruning methods such as TDDS (Zhang et al., 2024b), CCS (Zheng et al., 2023), and UNSEEN (Xu et al., 2025) further advance data-efficiency for training, but they remain single-distribution methods: their scoring functions are defined entirely on the training distribution. As such, they cannot exploit the contrast between the forget and retain distributions that drives distributional unlearning.

Remark 3 (Retain data assumption). *When no retain distribution is available, our objective collapses to selecting influential points within the forget distribution, which is more aligned with classical coresset construction. Our experiments indicate that such single-distribution methods are limited in low-divergence regimes: they emphasize representativeness within the forget distribution but cannot leverage the crucial contrast with the retain distribution that drives effective data removal. For this reason, we view acquiring or defining even a coarse proxy retain dataset (e.g., a general capabilities corpus) as an important practical consideration for applying distributional unlearning.*

| 486 487 488 489 490 491 492 | 486 487 488 489 490 491 492 | 486 487 488 489 490 491 492 | 486 487 488 489 490 491 492 | 486 487 488 489 490 491 492 |
|---|---|---|---|---|
| 486 487 488 489 490 491 492 | 486 487 488 489 490 491 492 | 486 487 488 489 490 491 492 | 486 487 488 489 490 491 492 | 486 487 488 489 490 491 492 |
| Unlearning | Selection Method | | | Savings |
| Method | Random | Coreset | Selective | |
| Retraining | 80 | 75 | 60 | 40% |
| Finetuning | 98 | 98 | 88 | 12% |
| NegGrad+ | 88 | 85 | 70 | 30% |
| SalUn | 68 | 75 | 55 | 45% |

| 486 487 488 489 490 491 492 | 486 487 488 489 490 491 492 | 486 487 488 489 490 491 492 |
|---|---|---|
| Selection | Unlearning Method | |
| Method | Retraining | Influence Func. |
| Selective | 15 | 18 |
| Random | 61 | 91 |
| Coreset | 63 | 93 |

Table 5: **Synergy with Sample-Level Unlearning.** Deletion budget (in %) required to reach: (*left*) 20% test accuracy on the CIFAR-10 forget class; (*right*) half the initial KL divergence in low-divergence Gaussians (Fig. 2, top left scenario). Our Selective removal is benchmarked against Random selection and a Coreset baseline across various sample-level unlearning methods. “Savings” indicates the relative reduction in size of selective removal from the full forget set.

5 CONCLUSION AND FUTURE WORK

Machine unlearning increasingly requires moving beyond individual record deletion to erase the influence of entire subpopulations. We tackled the central dilemma of this task: that full removal is computationally expensive, while naive partial removal is statistically inefficient. We find that a domain’s statistical influence is often concentrated in a small high-impact subset of its samples. We formalized this insight as *distributional unlearning*, a framework for selecting a small subset of data that optimally balances forgetting an unwanted distribution while preserving a desired one. Our theoretical analysis provided provable guarantees connecting this data-centric approach to downstream model performance, and our experiments validated that a selective, distance-based removal strategy is often more data-efficient than random or full removals across a range of tasks. While our work provides a foundation for selective data removal, we acknowledge its limitations, which point to important directions for future research below.

Distributional assumptions. Our finite-sample analysis provides strong guarantees but assumes Gaussian distributions; while our experiments show the core insights generalize qualitatively, bridging the gap between these theoretical bounds and the behavior on complex real-world data remains an open question. This distributional mismatch also helps explain the gap between the 82% data savings in our low-divergence synthetic setting and the still-significant 15–50% savings on real data. More fundamentally, our framework operates on samples that have already been identified as belonging to an unwanted subpopulation. This leads to an exciting extension of our work: because we show that only a small subset is needed for effective unlearning, this creates the potential for active identification systems that could help practitioners find these few, high-impact samples at a fraction of the cost of exhaustive annotation.

Data- to model-level guarantees. Moreover, our evaluation of unlearning is based on model performance degradation, which directly validates our theoretical log-loss guarantees. A privacy-centric evaluation could employ methods like Membership Inference attacks (Shokri et al., 2017) to formally verify that the unlearned model is indistinguishable from one retrained from scratch, representing another crucial avenue for future work. Conceptually, one could make a formal link between the (sample-level) certified (Guo et al., 2020) and distributional unlearning frameworks.

LLM fine-tuning applications. Beyond the foundational discriminative settings studied here, there is now a rapidly expanding line of work on data selection for large language model (LLM) instruction tuning. Classical instruction tuning (Wei et al., 2022), demonstrates that finetuning on curated instruction datasets can significantly improve generalization. More recent approaches focus on selecting high-quality subsets from a single instruction distribution to improve supervised fine-tuning (SFT) efficiency (Li et al., 2024a;b; Wang et al., 2025); see also the survey of Zhang et al. (2025). These methods aim to upweight instructive or representative examples for SFT, whereas our framework addresses a fundamentally different objective: distributional unlearning requires selecting a deletion subset that shifts a model’s behavior between two distributions. In this sense, our theory is model-agnostic and can serve as the selection layer for future (multimodal) LLM unlearning pipelines by operating directly on data representations (e.g., LLM embeddings) and respecting forget/retain distributional structure.

540 REPRODUCIBILITY STATEMENT
541542 We provide experimental reproducibility details in Appendix B. Moreover, we will release our code
543 publicly upon publication of the paper.
544545 LARGE LANGUAGE MODEL USAGE
546548 Large language models were used by the authors to aid or polish the writing of the paper. Authors
549 take full responsibility for the content.
550551 REFERENCES
552553 Youssef Allouah, Joshua Kazdan, Rachid Guerraoui, and Sanmi Koyejo. The utility and complexity
554 of in- and out-of-distribution machine unlearning. In *The Thirteenth International Conference on*
555 *Learning Representations*, 2025.556 Tiago A. Almeida, José M. Gómez Hidalgo, and Akebo Yamakami. Contributions to the study of
557 sms spam filtering: New collection and results. In *Proceedings of the 11th ACM Symposium on*
558 *Document Engineering*, pp. 3–10. ACM, 2011.559 Arindam Banerjee, Srujana Merugu, Inderjit S Dhillon, and Joydeep Ghosh. Clustering with breg-
560 man divergences. *Journal of machine learning research*, 6(Oct):1705–1749, 2005.
561562 Nora Belrose, David Schneider-Joseph, Shauli Ravfogel, Ryan Cotterell, Edward Raff, and Stella
563 Biderman. Leace: Perfect linear concept erasure in closed form. *Advances in Neural Information*
564 *Processing Systems*, 36:66044–66063, 2023.565 Shai Ben-David, John Blitzer, Koby Crammer, Alex Kulesza, Fernando Pereira, and Jennifer Wort-
566 man Vaughan. A theory of learning from different domains. *Machine learning*, 79:151–175,
567 2010.568 Dimitri P Bertsekas. Nonlinear programming. *Journal of the Operational Research Society*, 48(3):
569 38–39, 1997.
570571 David M Blei, Andrew Y Ng, and Michael I Jordan. Latent dirichlet allocation. *Journal of machine*
572 *Learning research*, 3(Jan):993–1022, 2003.573 Lucas Bourtoule, Varun Chandrasekaran, Christopher A Choquette-Choo, Hengrui Jia, Adelin
574 Travers, Baiwu Zhang, David Lie, and Nicolas Papernot. Machine unlearning. In *2021 IEEE*
575 *Symposium on Security and Privacy (SP)*, pp. 141–159. IEEE, 2021.
576577 Eli Chien, Haoyu Peter Wang, Ziang Chen, and Pan Li. Langevin unlearning: A new perspective
578 of noisy gradient descent for machine unlearning. In *The Thirty-eighth Annual Conference on*
579 *Neural Information Processing Systems*, 2024. URL <https://openreview.net/forum?id=3LKuC8rbyV>.
580581 Rishav Chourasia and Neil Shah. Forget unlearning: Towards true data-deletion in machine learning.
582 In *International Conference on Machine Learning*, pp. 6028–6073. PMLR, 2023.
583584 Yanai Lazar and Yoav Goldberg. Adversarial removal of demographic attributes from text data. In
585 *Proceedings of the 2018 Conference on Empirical Methods in Natural Language Processing*, pp.
586 11–21, 2018.
587588 Ronen Eldan and Mark Russinovich. Who’s harry potter? approximate unlearning in llms. *arXiv*
589 *preprint arXiv:2310.02238*, 2023.
590591 Chongyu Fan, Jiancheng Liu, Yihua Zhang, Eric Wong, Dennis Wei, and Sijia Liu. Salun: Em-
592 powering machine unlearning via gradient-based weight saliency in both image classification and
593 generation. In *The Twelfth International Conference on Learning Representations*, 2024. URL
<https://openreview.net/forum?id=gn0mIhQGNM>.

594 Claudio Gentile, Zhilei Wang, and Tong Zhang. Fast rates in pool-based batch active learning.
 595 *Journal of Machine Learning Research*, 25(262):1–42, 2024.
 596

597 Chuan Guo, Tom Goldstein, Awni Hannun, and Laurens Van Der Maaten. Certified data removal
 598 from machine learning models. In *International Conference on Machine Learning*, pp. 3832–
 599 3842. PMLR, 2020.

600 Zachary Izzo, Mary Anne Smart, Kamalika Chaudhuri, and James Zou. Approximate data dele-
 601 tion from machine learning models. In *International Conference on Artificial Intelligence and*
 602 *Statistics*, pp. 2008–2016. PMLR, 2021.

603

604 Divyansh Kaushik, Eduard Hovy, and Zachary Lipton. Learning the difference that makes a differ-
 605 ence with counterfactually-augmented data. In *International Conference on Learning Represen-
 606 tations*, 2020. URL <https://openreview.net/forum?id=Sk1gs0NFvr>.

607 Krishnateja Killamsetty, Sivasubramanian Durga, Ganesh Ramakrishnan, Abir De, and Rishabh
 608 Iyer. Grad-match: Gradient matching based data subset selection for efficient deep model training.
 609 In *International Conference on Machine Learning*, pp. 5464–5474. PMLR, 2021.

610

611 Sangamesh Kodge, Gobinda Saha, and Kaushik Roy. Deep unlearning: Fast and efficient gradient-
 612 free class forgetting. *Transactions on Machine Learning Research*, 2024. ISSN 2835-8856. URL
 613 <https://openreview.net/forum?id=BmI5p6wBi0>.

614 Anastasia Koloskova, Youssef Allouah, Animesh Jha, Rachid Guerraoui, and Sanmi Koyejo. Certi-
 615 fied unlearning for neural networks. In *Forty-second International Conference on Machine Learn-
 616 ing*, 2025. URL <https://openreview.net/forum?id=3rWQ1V3s1I>.

617

618 Alex Krizhevsky, Vinod Nair, and Geoffrey Hinton. The cifar-10 dataset. *online*: <http://www.cs.toronto.edu/kriz/cifar.html>, 55(5), 2014.

619

620 Meghdad Kurmanji, Peter Triantafillou, Jamie Hayes, and Eleni Triantafillou. Towards unbounded
 621 machine unlearning. *Advances in Neural Information Processing Systems*, 36, 2024.

622

623 Ming Li, Yong Zhang, Zhitao Li, Jiahui Chen, Lichang Chen, Ning Cheng, Jianzong Wang, Tianyi
 624 Zhou, and Jing Xiao. From quantity to quality: Boosting llm performance with self-guided data
 625 selection for instruction tuning. In *Proceedings of the 2024 Conference of the North American
 626 Chapter of the Association for Computational Linguistics: Human Language Technologies (Vol-
 627 ume 1: Long Papers)*, pp. 7602–7635, 2024a.

628

629 Yunshui Li, Binyuan Hui, Xiaobo Xia, Jiaxi Yang, Min Yang, Lei Zhang, Shuzheng Si, Ling-Hao
 630 Chen, Junhao Liu, Tongliang Liu, et al. One-shot learning as instruction data prospector for large
 631 language models. In *Proceedings of the 62nd Annual Meeting of the Association for Compu-
 632 tational Linguistics (Volume 1: Long Papers)*, pp. 4586–4601, 2024b.

633

634 Ken Liu, Christopher A. Choquette-Choo, Matthew Jagielski, Peter Kairouz, Sanmi Koyejo, Percy
 635 Liang, and Nicolas Papernot. Language models may verbatim complete text they were not ex-
 636 plicitly trained on. In *Forty-second International Conference on Machine Learning*, 2025. URL
 637 <https://openreview.net/forum?id=bLcXkIasck>.

638

639 Baharan Mirzasoleiman, Jeff Bilmes, and Jure Leskovec. Coresets for data-efficient training of
 640 machine learning models. In *International Conference on Machine Learning*, pp. 6950–6960.
 641 PMLR, 2020.

642

643 Seth Neel, Aaron Roth, and Saeed Sharifi-Malvajerdi. Descent-to-delete: Gradient-based methods
 644 for machine unlearning. In *Algorithmic Learning Theory*, pp. 931–962. PMLR, 2021.

645

646 Shauli Ravfogel, Yair Elazar, and Yoav Goldberg. Null it out: Guarding protected attributes by
 647 iterative nullspace projection. In *Proceedings of the 2020 Conference on Empirical Methods in
 648 Natural Language Processing (EMNLP)*, pp. 7231–7245, 2020.

649

650 Shai Shalev-Shwartz and Shai Ben-David. *Understanding machine learning: From theory to algo-
 651 rithms*. Cambridge university press, 2014.

648 Reza Shokri, Marco Stronati, Congzheng Song, and Vitaly Shmatikov. Membership inference at-
 649 tacks against machine learning models. In *2017 IEEE symposium on security and privacy (SP)*,
 650 pp. 3–18. IEEE, 2017.

651

652 Akash Srivastava and Charles Sutton. Autoencoding variational inference for topic models. In
 653 *International Conference on Learning Representations*, 2017. URL <https://openreview.net/forum?id=BybtVK91g>.

654

655 Ayush K Tarun, Vikram S Chundawat, Murari Mandal, and Mohan Kankanhalli. Fast yet effective
 656 machine unlearning. *IEEE Transactions on Neural Networks and Learning Systems*, 2023.

657

658 Martin Van Waerebeke, Marco Lorenzi, Giovanni Neglia, and Kevin Scaman. When to forget? com-
 659 plexity trade-offs in machine unlearning. In *Forty-second International Conference on Machine*
 660 *Learning*, 2025. URL <https://openreview.net/forum?id=uEUIeIrRPv>.

661 Martin J Wainwright, Michael I Jordan, et al. Graphical models, exponential families, and variational
 662 inference. *Foundations and Trends® in Machine Learning*, 1(1–2):1–305, 2008.

663

664 Shaobo Wang, Xiangqi Jin, Ziming Wang, Jize Wang, Jiajun Zhang, Kaixin Li, Zichen Wen, Zhong
 665 Li, Conghui He, Xuming Hu, and Linfeng Zhang. Data whisperer: Efficient data selection for
 666 task-specific LLM fine-tuning via few-shot in-context learning. In Wanxiang Che, Joyce Nabende,
 667 Ekaterina Shutova, and Mohammad Taher Pilehvar (eds.), *Proceedings of the 63rd Annual Meet-
 668 ing of the Association for Computational Linguistics (Volume 1: Long Papers)*, pp. 23287–23305,
 669 Vienna, Austria, July 2025. Association for Computational Linguistics. ISBN 979-8-89176-
 670 251-0. doi: 10.18653/v1/2025.acl-long.1135. URL <https://aclanthology.org/2025.acl-long.1135/>.

671

672 Jason Wei, Maarten Bosma, Vincent Zhao, Kelvin Guu, Adams Wei Yu, Brian Lester, Nan Du, An-
 673 drew M Dai, and Quoc V Le. Finetuned language models are zero-shot learners. In *International*
 674 *Conference on Learning Representations*, 2022.

675

676 Furui Xu, Shaobo Wang, Luo Zhongwei, and Linfeng Zhang. Rethinking dataset pruning from a
 677 generalization perspective. In *The Future of Machine Learning Data Practices and Repositories
 at ICLR 2025*, 2025.

678

679 Binchi Zhang, Yushun Dong, Tianhao Wang, and Jundong Li. Towards certified unlearning for deep
 680 neural networks. In *Proceedings of the 41st International Conference on Machine Learning*, pp.
 681 58800–58818, 2024a.

682

683 Bolin Zhang, Jiahao Wang, Qianlong Du, Jiajun Zhang, Zhiying Tu, and Dianhui Chu. A survey on
 684 data selection for llm instruction tuning. *Journal of Artificial Intelligence Research*, 83, 2025.

685

686 Xin Zhang, Jiawei Du, Yunsong Li, Weiying Xie, and Joey Tianyi Zhou. Spanning training
 687 progress: Temporal dual-depth scoring (tdds) for enhanced dataset pruning. In *Proceedings of the
 688 IEEE/CVF Conference on Computer Vision and Pattern Recognition*, pp. 26223–26232, 2024b.

689

690 Haizhong Zheng, Rui Liu, Fan Lai, and Atul Prakash. Coverage-centric coresset selection for high
 691 pruning rates. In *The Eleventh International Conference on Learning Representations*, 2023.

692

693

694

695

696

697

698

699

700

701

702 **A PROOFS**

703 **A.1 PARETO FRONTIER**

704 **Proposition 1** (Pareto Frontier). *Let p_1, p_2 be two distributions in \mathcal{P} , the class of Gaussian distributions with shared positive covariance. The Pareto frontier of (α, ε) values achievable in \mathcal{P} is:*

$$705 \quad \text{PF}(p_1, p_2; \mathcal{P}) = \left\{ \left(\alpha, \left(\sqrt{\alpha} - \sqrt{\text{KL}(p_1 \| p_2)} \right)^2 \right) : \alpha \geq \text{KL}(p_1 \| p_2) \right\}.$$

711 *Proof.* For simplicity, we consider univariate Gaussians with shared variance. For d -dimensional Gaussians with covariance $\Sigma \in \mathbb{R}^{d \times d}$, the same result holds after replacing squared error by the Mahalanobis distance $\|x - \mu\|_{\Sigma^{-1}}^2$ (see Proposition 4).

714 Let $p = \mathcal{N}(\mu, \sigma^2) \in \mathcal{P}$. Since all distributions in \mathcal{P} share the same variance, the KL divergence from p_i to p is:

$$715 \quad \text{KL}(p_i \| p) = \frac{(\mu_i - \mu)^2}{2\sigma^2}, \quad i = 1, 2.$$

718 Fix $\alpha \geq \text{KL}(p_1 \| p_2)$. We want to compute the minimal possible ε achievable under the constraint $\text{KL}(p_1 \| p) \geq \alpha$. Define this minimum as:

$$721 \quad \varepsilon_*(\alpha) := \min_{\mu \in \mathbb{R}, (\mu - \mu_1)^2 \geq 2\sigma^2 \alpha} \frac{(\mu_2 - \mu)^2}{2\sigma^2}.$$

723 This is a one-dimensional quadratic minimization problem subject to a quadratic inequality constraint. The feasible set is:

$$725 \quad \mu \in (-\infty, \mu_1 - \sigma\sqrt{2\alpha}] \cup [\mu_1 + \sigma\sqrt{2\alpha}, \infty).$$

727 We minimize $(\mu_2 - \mu)^2$ over this set. This yields two cases:

729 • If $\mu_2 \in [\mu_1 - \sigma\sqrt{2\alpha}, \mu_1 + \sigma\sqrt{2\alpha}]$, then the closest feasible points are the endpoints. The
730 minimizing value of μ is:

$$731 \quad \mu = \mu_1 + \text{sign}(\mu_2 - \mu_1) \cdot \sigma\sqrt{2\alpha},$$

733 and the resulting divergence is:

$$734 \quad \varepsilon_*(\alpha) = \frac{(\mu_2 - \mu_1 - \text{sign}(\mu_2 - \mu_1) \cdot \sigma\sqrt{2\alpha})^2}{2\sigma^2}.$$

737 • If μ_2 already lies in the feasible set, i.e., $|\mu_2 - \mu_1| \geq \sigma\sqrt{2\alpha}$, then we can choose $\mu = \mu_2$,
738 yielding $\varepsilon_*(\alpha) = 0$.

740 Thus, for all $\alpha \geq 0$:

$$741 \quad \varepsilon_*(\alpha) = \frac{[(|\mu_2 - \mu_1| - \sigma\sqrt{2\alpha})_+]^2}{2\sigma^2},$$

744 where $(x)_+ = \max\{x, 0\}$. Let $\Delta := |\mu_2 - \mu_1|$, and recall that $\text{KL}(p_1 \| p_2) = \frac{\Delta^2}{2\sigma^2}$. Then:

$$745 \quad \Delta = \sigma\sqrt{2\text{KL}(p_1 \| p_2)}.$$

747 Substituting into $\varepsilon_*(\alpha)$:

$$748 \quad \varepsilon_*(\alpha) = \left(\sqrt{\alpha} - \sqrt{\text{KL}(p_1 \| p_2)} \right)^2, \quad \text{for } \alpha \geq \text{KL}(p_1 \| p_2).$$

751 Finally, note that any pair (α, ε) with $\alpha < \text{KL}(p_1 \| p_2)$ satisfies $\varepsilon_*(\alpha) = 0$, hence is dominated by
752 $(\text{KL}(p_1 \| p_2), 0)$. Therefore, the Pareto optimal points are exactly:

$$753 \quad \left\{ \left(\alpha, \left(\sqrt{\alpha} - \sqrt{\text{KL}(p_1 \| p_2)} \right)^2 \right) : \alpha \geq \text{KL}(p_1 \| p_2) \right\},$$

755 as claimed. □

756 Next, we show that a qualitatively similar result holds more generally for any exponential-family
 757 member.

758 **Theorem 4** (Pareto Frontier–Exponential Families). *Let (\mathcal{X}, μ) be a measurable space and let*

$$760 \quad \mathcal{P} = \{p_\theta(x) = h(x) \exp(\theta^\top T(x) - A(\theta)) : \theta \in \Theta \subset \mathbb{R}^d\}$$

761 *be a regular minimal exponential family (carrier $h > 0$, sufficient statistic $T: \mathcal{X} \rightarrow \mathbb{R}^d$,
 762 log-partition A). Fix $p_i(x) = p_{\theta_i}(x)$, $i = 1, 2$, and $\alpha \geq 0$. Define $v(\alpha) =$
 763 $\inf_{\theta \in \Theta} \{KL(p_2 \| p_\theta) \mid KL(p_1 \| p_\theta) \geq \alpha\}$, where $KL(q \| p) = \int q \log(q/p) d\mu$. Then:*

765 (i) *The Pareto frontier for points in \mathcal{P} is*

$$766 \quad PF(p_1, p_2; \mathcal{P}) = \{(\alpha, v(\alpha)) : \alpha \geq KL(p_1 \| p_2)\},$$

767 *where $v(\alpha) = KL(p_2 \| p_1) + \alpha + \frac{1}{\lambda^* - 1}(\theta_2 - \theta_1)^\top (\mathbb{E}_{p_2}[T] - \mathbb{E}_{p_1}[T])$, and λ^* is the unique
 768 scalar in $(0, 1)$ such that the distribution $p^* \in \mathcal{P}$ of mean $\mathbb{E}_{p^*}[T] = \frac{\lambda^* \mathbb{E}_{p_1}[T] - \mathbb{E}_{p_2}[T]}{\lambda^* - 1}$
 769 satisfies $KL(p_1 \| p^*) = \alpha$.*

770 (ii) *(Gaussian case) If $\mathcal{P} = \{\mathcal{N}(\mu, \Sigma) : \mu \in \mathbb{R}^d\}$ with fixed $\Sigma \succ 0$, then for $\alpha \geq KL(p_1 \| p_2)$:*

$$771 \quad v(\alpha) = (\sqrt{\alpha} - \sqrt{KL(p_1 \| p_2)})^2.$$

772 *Proof.* In this proof, for a fixed $\alpha \geq 0$, we study the optimal value

$$773 \quad v(\alpha) = \inf_{\theta \in \Theta} \{KL(p_2 \| p_\theta) \mid KL(p_1 \| p_\theta) \geq \alpha\}.$$

774 This enables characterizing the Pareto frontier of feasible (α, ε) trade-offs. Below, we focus on
 775 the non-trivial case $\alpha > KL(p_1 \| p_2)$. Indeed, in the case $\alpha \leq KL(p_1 \| p_2)$, the problem above's
 776 unconstrained minimizer p_2 is a feasible solution, so that $v(\alpha) = 0$ for all $\alpha \leq KL(p_1 \| p_2)$.

777 **Reparametrization and KKT.** First, we recall the expression of the KL divergence in exponential
 778 families as a Bregman divergence. For any $\theta', \theta \in \Theta$ one has

$$779 \quad KL(p_{\theta'} \| p_\theta) = A(\theta) - A(\theta') - (\theta - \theta')^\top \nabla A(\theta').$$

780 We let

$$781 \quad f(\theta) = KL(p_2 \| p_\theta), \quad g(\theta) = KL(p_1 \| p_\theta).$$

782 Both are continuously differentiable on the open set Θ . The feasible set $\{g(\theta) \geq \alpha\}$ is nonconvex,
 783 so we check linear independence constraint qualification (LICQ, Bertsekas (1997)) at any minimizer
 784 θ^* . To do so, we recall (see Wainwright et al. (2008)) that for exponential families $\nabla A(\theta) = \mathbb{E}_{p_\theta}[T]$
 785 for any $\theta \in \Theta$, so that

$$786 \quad \nabla g(\theta) = -\nabla A(\theta_1) + \nabla A(\theta) = -\mathbb{E}_{p_1}[T] + \mathbb{E}_{p_\theta}[T].$$

787 Minimality of the exponential family ensures $\mathbb{E}_{p_\theta}[T]$ is injective Wainwright et al. (2008). This
 788 together with the fact that $p_1 \neq p_\theta$ for any feasible θ , since $\alpha > 0$, implies that $\nabla g(\theta^*) \neq 0$ and
 789 LICQ holds.

790 Next, we form the Lagrangian

$$791 \quad \mathcal{L}(\theta, \lambda) = f(\theta) - \lambda(g(\theta) - \alpha), \quad \lambda \geq 0.$$

792 Since LICQ holds, KKT conditions are necessary Bertsekas (1997) for any minimizer θ^* . Hence,
 793 stationarity ($\nabla_\theta \mathcal{L} = 0$) gives

$$794 \quad \nabla f(\theta^*) = \lambda \nabla g(\theta^*).$$

795 Given that we had derived $\nabla_\theta KL(p_i \| p_\theta) = -\mathbb{E}_{p_i}[T] + \mathbb{E}_{p_\theta}[T]$, we obtain

$$796 \quad -\mathbb{E}_{p_2}[T] + \mathbb{E}_{p^*}[T] = \lambda(-\mathbb{E}_{p_1}[T] + \mathbb{E}_{p^*}[T]),$$

797 hence $(1 - \lambda) \mathbb{E}_{p^*}[T] = \mathbb{E}_{p_2}[T] - \lambda \mathbb{E}_{p_1}[T]$. Observe that we must have $\lambda \neq 1$, as otherwise
 798 $\mathbb{E}_{p_2}[T] = \mathbb{E}_{p_1}[T]$, but this contradicts the fact that $p_1 \neq p_2$ given that $\mathbb{E}_{p_\theta}[T]$ is injective for
 799 minimal exponential families Wainwright et al. (2008). Therefore, we have the following:

$$800 \quad \mathbb{E}_{p^*}[T] = \frac{\lambda \mathbb{E}_{p_1}[T] - \mathbb{E}_{p_2}[T]}{\lambda - 1}.$$

Now, we observe that the inequality constraint must be active. Otherwise, the minimizer lies in the interior of the feasible set and is thus a local minimum of the unconstrained problem. The latter admits p_2 as a unique minimizer, so the minimizer at hand must be p_2 but this is not feasible since we assume $\text{KL}(p_1\|p_2) < \alpha$. Therefore, the minimizer must lie at the boundary of the feasible set, and the inequality constraint is active. That is, we have $g(\theta^*) = \alpha$.

Optimal value. We are now ready to derive the expression of the optimal value:

$$v(\alpha) = f(\theta^*) = \text{KL}(p_2\|p^*).$$

We use the following classical Pythagorean-type identity for Bregman divergences (see, e.g., Banerjee et al. (2005)):

$$\text{KL}(p_2\|p^*) = \text{KL}(p_2\|p_1) + \text{KL}(p_1\|p^*) + (\theta_2 - \theta_1)^\top (\nabla A(\theta_1) - \nabla A(\theta^*)).$$

Now, consider the aforementioned KKT multiplier $\lambda > 0, \lambda \neq 1$ such that $\nabla A(\theta^*) = \mathbb{E}_{p^*}[T] = \frac{\lambda \mathbb{E}_{p_1}[T] - \mathbb{E}_{p_2}[T]}{\lambda - 1} = \frac{\lambda \nabla A(\theta_1) - \nabla A(\theta_2)}{\lambda - 1}$ as well as $\text{KL}(p_1\|p^*) = g(\theta^*) = \alpha$. We thus get

$$\begin{aligned} v(\alpha) &= \text{KL}(p_2\|p^*) = \text{KL}(p_2\|p_1) + \text{KL}(p_1\|p^*) + (\theta_2 - \theta_1)^\top (\nabla A(\theta_1) - \nabla A(\theta^*)) \\ &= \text{KL}(p_2\|p_1) + \text{KL}(p_1\|p^*) + \frac{1}{\lambda - 1} (\theta_2 - \theta_1)^\top (\nabla A(\theta_2) - \nabla A(\theta_1)) \\ &= \text{KL}(p_2\|p_1) + \alpha + \frac{1}{\lambda - 1} (\theta_2 - \theta_1)^\top (\nabla A(\theta_2) - \nabla A(\theta_1)). \end{aligned}$$

We now again use that $\nabla A(\theta) = \mathbb{E}_{p_\theta}[T]$ for all $\theta \in \Theta$. We then obtain:

$$v(\alpha) = \text{KL}(p_2\|p_1) + \alpha + \frac{1}{\lambda - 1} (\theta_2 - \theta_1)^\top (\mathbb{E}_{p_2}[T] - \mathbb{E}_{p_1}[T]). \quad (3)$$

Uniqueness of λ . We now show that there is a unique KKT multiplier λ for the optimal solution. We recall that $\lambda > 0$ is such that $\lambda \neq 1$ and:

$$\mathbb{E}_{p^*}[T] = \frac{\lambda \mathbb{E}_{p_1}[T] - \mathbb{E}_{p_2}[T]}{\lambda - 1} \quad g(\theta^*) = \text{KL}(p_1\|p^*) = \alpha.$$

Above, the first equation uniquely defines the distribution p^* , by minimality of the family, and we now show that there is only a unique λ of interest such that the second equations above holds.

Let $\theta^*(\lambda)$ be the unique (by minimality) parameter such that $\mathbb{E}_{p^*}[T] = \frac{\lambda \mathbb{E}_{p_1}[T] - \mathbb{E}_{p_2}[T]}{\lambda - 1}$. We define

$$H(\lambda) := \text{KL}(p_1\|p^*) = A(\theta^*) - A(\theta_1) - (\theta^* - \theta_1)^\top \nabla A(\theta_1)$$

Taking the derivative above, we get

$$\frac{dH}{d\lambda}(\lambda) = (\nabla A(\theta^*) - \nabla A(\theta_1))^\top \frac{d\theta^*}{d\lambda}(\lambda).$$

We again use that

$$\nabla A(\theta^*) = \mathbb{E}_{p^*}[T] = \frac{\lambda \mathbb{E}_{p_1}[T] - \mathbb{E}_{p_2}[T]}{\lambda - 1} = \frac{\lambda \nabla A(\theta_1) - \nabla A(\theta_2)}{\lambda - 1}.$$

First, replacing in the previous derivative equation, we obtain:

$$\frac{dH}{d\lambda}(\lambda) = (\nabla A(\theta^*) - \nabla A(\theta_1))^\top \frac{d\theta^*}{d\lambda}(\lambda) = \frac{1}{\lambda - 1} (\nabla A(\theta_1) - \nabla A(\theta_2))^\top \frac{d\theta^*}{d\lambda}(\lambda).$$

Second, taking the derivative with respect to λ in the expression of $\nabla A(\theta^*)$ yields:

$$\nabla^2 A(\theta^*) \cdot \frac{d\theta^*}{d\lambda}(\lambda) = \frac{1}{(\lambda - 1)^2} (\nabla A(\theta_1) - \nabla A(\theta_2)).$$

We observe that the Fisher information matrix $\nabla^2 A(\theta^*)$ is positive definite since the family is regular. Multiplying by the inverse of the latter then yields:

$$\frac{d\theta^*}{d\lambda}(\lambda) = \frac{1}{(\lambda - 1)^2} \nabla^2 A(\theta^*)^{-1} (\nabla A(\theta_1) - \nabla A(\theta_2)).$$

864 Plugging the above in the latest expression of the derivative of H yields:
 865

$$\begin{aligned} 866 \frac{dH}{d\lambda}(\lambda) &= \frac{1}{\lambda-1}(\nabla A(\theta_1) - \nabla A(\theta_2))^\top \frac{d\theta^*}{d\lambda}(\lambda) \\ 867 \\ 868 &= \frac{1}{(\lambda-1)^3}(\nabla A(\theta_1) - \nabla A(\theta_2))^\top \nabla^2 A(\theta^*)^{-1}(\nabla A(\theta_1) - \nabla A(\theta_2)). \\ 869 \end{aligned}$$

870 Since the matrix $\nabla^2 A(\theta^*)$ is positive definite by regularity of the family, the corresponding quadratic
 871 form above is positive (recall $\theta_1 \neq \theta_2$), and the sign of the derivative is that of $\lambda - 1$. Therefore,
 872 H is decreasing on $(0, 1)$ and increasing on $(1, +\infty)$. It is straightforward to check that $H(0^+) =$
 873 $\text{KL}(p_1 \| p_2)$, $H(1^-) = H(1^+) = +\infty$, and $H(+\infty) = 0$. Since $\text{KL}(p_1 \| p_2) < \alpha$ by assumption,
 874 there exists a unique $\lambda^* \in (0, 1)$ such that $H(\lambda^*) = \alpha$ and a unique $\lambda_1^* > 1$ such that $H(\lambda_1^*) = \alpha$.
 875

876 We now discard λ_1^* thanks to the expression of the optimal value expression (3). Indeed, the second
 877 term in (3) is positive for $\lambda_1^* > 1$ and $(\theta_2 - \theta_1)^\top (\mathbb{E}_{p_2}[T] - \mathbb{E}_{p_1}[T]) = (\theta_2 - \theta_1)^\top (\nabla A(\theta_2) -$
 878 $\nabla A(\theta_1)) > 0$ by strict convexity of A and the fact that $p_1 \neq p_2$. On the other hand, this same second
 879 term is negative for λ_* since $\lambda_* < 1$. Therefore, the optimal value is smaller for the choice of λ^* , so
 880 that:
 881

$$v(\alpha) = \text{KL}(p_2 \| p_1) + \alpha + \frac{1}{\lambda^* - 1}(\theta_2 - \theta_1)^\top (\mathbb{E}_{p_2}[T] - \mathbb{E}_{p_1}[T]), \quad (4)$$

882 where λ^* is the unique scalar in $(0, 1)$ such that:
 883

$$\mathbb{E}_{p^*}[T] = \frac{\lambda^* \mathbb{E}_{p_1}[T] - \mathbb{E}_{p_2}[T]}{\lambda^* - 1} \quad g(\theta^*) = \text{KL}(p_1 \| p^*) = \alpha.$$

884 Finally, we note that $v(\alpha)$ is non-decreasing by definition; increasing α shrinks the feasible set. Also,
 885 we recall that $v(\alpha) = 0$ for all $\alpha < \text{KL}(p_1 \| p_2)$, i.e., all trade-offs (α, ε) with $\alpha < \text{KL}(p_1 \| p_2), \varepsilon > 0$
 886 are dominated by $(\text{KL}(p_1 \| p_2), 0)$. Therefore, we conclude that the pareto frontier is given by:
 887

$$\text{PF}(p_1, p_2; \mathcal{P}) = \left\{ (\alpha, v(\alpha)) : \alpha \geq \text{KL}(p_1 \| p_2) \right\}.$$

888 **Gaussian case.** For $p_\mu = \mathcal{N}(\mu, \Sigma)$ one has $T(x) = x$, $E_{p_\mu}[T] = \mu$, and
 889

$$\text{KL}(p_i \| p_\mu) = \frac{1}{2}(\mu_i - \mu)^\top \Sigma^{-1}(\mu_i - \mu).$$

890 By the conditions on λ^* we have
 891

$$\mu^* = \frac{\lambda^* \mu_1 - \mu_2}{\lambda^* - 1}, \quad \text{KL}(p_1 \| p_{\mu^*}) = \alpha.$$

892 Using the KL divergence expression for Gaussians $\mathcal{N}(\mu, \Sigma)$ (recall $\text{KL}(\mathcal{N}(\mu_1, \Sigma), \mathcal{N}(\mu_2, \Sigma)) =$
 893 $\frac{1}{2}(\mu_1 - \mu_2)^\top \Sigma^{-1}(\mu_1 - \mu_2)$), we get
 894

$$\mu_1 - \mu^* = \frac{\mu_2 - \mu_1}{\lambda^* - 1}, \quad \alpha = \frac{\text{KL}(p_1 \| p_2)}{(\lambda^* - 1)^2}.$$

895 Solving for $\lambda^* \in (0, 1)$ yields $\lambda^* = 1 - \sqrt{\text{KL}(p_1 \| p_2) / \alpha}$ and
 896

$$\mu^* = \mu_1 + \sqrt{\frac{\alpha}{\text{KL}(p_1 \| p_2)}}(\mu_2 - \mu_1).$$

897 Thus, direct computations yield
 898

$$v(\alpha) = \frac{1}{2} \left(\|\mu_2 - \mu_1\|_{\Sigma^{-1}} - \sqrt{2\alpha} \right)^2 = (\sqrt{\text{KL}(p_1 \| p_2)} - \sqrt{\alpha})^2,$$

899 with $v(\alpha) = 0$ if $\alpha \leq \text{KL}(p_1 \| p_2)$. This concludes the proof. \square
 900

901 **Discussion.** In Proposition 4 we show that, in any regular exponential family, the trade-off between
 902 removal (α) and preservation (ε) can be quantified. This yields a removal-preservation trade-off
 903 curve that faithfully reproduces the shared-covariance Gaussian Pareto frontier—namely the familiar
 904 $(\sqrt{\alpha} - \sqrt{D})^2$ parabola—while in other families it gives an explicit but generally non-algebraic trade-
 905 off curve.
 906

918 A.2 PREDICTIVE PERFORMANCE
919

920 **Proposition 2.** Let h minimize $\mathcal{L}(h; p)$, and let h_1, h_2 be optimal predictors under $p_1, p_2 \in \mathcal{P}$,
921 respectively. If p satisfies (α, ε) -distributional unlearning with respect to (p_1, p_2) , then:

$$922 \quad \mathcal{L}(h; p_1) - \mathcal{L}(h_1; p_1) \geq \alpha - \delta_1, \quad \mathcal{L}(h; p_2) - \mathcal{L}(h_2; p_2) \leq \varepsilon - \delta_2, \quad (2)$$

924 where $\delta_1 := \text{KL}(p_{1,X} \| p_X)$, $\delta_2 := \text{KL}(p_{2,X} \| p_X)$ denote the marginal KL divergence over inputs.
925

926 *Proof.* Let $h(y | x) := h(x)(y)$ denote the conditional distribution defined by the hypothesis h , and
927 suppose h minimizes the expected log-loss under p . Since $\ell(y, q) = -\log q(y)$ is a strictly proper
928 scoring rule, the unique minimizer of $\mathcal{L}(h; p)$ is the true conditional distribution $h(x) = p(\cdot | x)$,
929 where $p(x, y) = p^X(x)p(y | x)$.

930 We begin by analyzing the expected log-loss of this hypothesis under an arbitrary distribution q over
931 $\mathcal{X} \times \mathcal{Y}$:

$$932 \quad \mathcal{L}(h; q) = \mathbb{E}_{(x,y) \sim q}[-\log h(y | x)] = \mathbb{E}_{x \sim q^X} \mathbb{E}_{y \sim q(\cdot | x)}[-\log p(y | x)],$$

934 where q^X denotes the marginal distribution of x under q , and $q(\cdot | x)$ the corresponding conditional.
935

936 Now recall the standard identity for any two conditional distributions $q(\cdot | x)$ and $p(\cdot | x)$:

$$937 \quad \mathbb{E}_{y \sim q(\cdot | x)}[-\log p(y | x)] = \text{KL}(q(y | x) \| p(y | x)) + H(q(y | x)),$$

939 where $H(q(y | x)) = \mathbb{E}_{y \sim q(\cdot | x)}[-\log q(y | x)]$ is the Shannon entropy of the label distribution
940 under q for fixed x .

941 Taking the expectation over $x \sim q^X$, we get:

$$942 \quad \begin{aligned} \mathcal{L}(h; q) &= \mathbb{E}_{x \sim q^X} [\text{KL}(q(y | x) \| p(y | x)) + H(q(y | x))] \\ 944 &= \mathbb{E}_{x \sim q^X} \text{KL}(q(y | x) \| p(y | x)) + \mathbb{E}_{x \sim q^X} H(q(y | x)). \end{aligned}$$

945 The second term is the expected entropy, which corresponds to the Bayes-optimal risk under q :

$$947 \quad \mathcal{L}(h_q^*; q) := \inf_{h'} \mathcal{L}(h'; q) = \mathbb{E}_{x \sim q^X} H(q(y | x)). \quad (5)$$

949 Next, we relate the expected conditional KL term to the total KL divergence between the joint
950 distributions. Using the chain rule for KL divergence, we have:

$$952 \quad \text{KL}(q \| p) = \text{KL}(q^X \| p^X) + \mathbb{E}_{x \sim q^X} \text{KL}(q(y | x) \| p(y | x)). \quad (6)$$

954 This decomposition holds generally for joint distributions with conditional factorizations. Solving
955 for the conditional KL term, we obtain:

$$957 \quad \mathbb{E}_{x \sim q^X} \text{KL}(q(y | x) \| p(y | x)) = \text{KL}(q \| p) - \text{KL}(q^X \| p^X). \quad (7)$$

958 Substituting the above into the expression for $\mathcal{L}(h; q)$ and using (5), we get:

$$960 \quad \mathcal{L}(h; q) = \text{KL}(q \| p) - \text{KL}(q^X \| p^X) + \mathcal{L}(h_q^*; q). \quad (8)$$

962 We now apply this to $q = p_1$ and $q = p_2$, noting that p satisfies (α, ε) -distributional unlearning, i.e.,
963 $\text{KL}(p_1 \| p) \geq \alpha$ and $\text{KL}(p_2 \| p) \leq \varepsilon$.
964

965 For p_1 , we define $\delta_1 := \text{KL}(p_1^X \| p^X)$ and compute:

$$966 \quad \mathcal{L}(h; p_1) - \mathcal{L}(h_1; p_1) = \text{KL}(p_1 \| p) - \text{KL}(p_1^X \| p^X) = \text{KL}(p_1 \| p) - \delta_1 \geq \alpha - \delta_1.$$

968 For p_2 , define $\delta_2 := \text{KL}(p_2^X \| p^X)$ and similarly compute:

$$970 \quad \mathcal{L}(h; p_2) - \mathcal{L}(h_2; p_2) = \text{KL}(p_2 \| p) - \text{KL}(p_2^X \| p^X) = \text{KL}(p_2 \| p) - \delta_2 \leq \varepsilon - \delta_2.$$

971 This completes the proof. \square

972 A.3 RANDOM REMOVAL
973974 **Lemma 5** (Finite-sample concentration). *Let $\hat{\mu}$ be the empirical mean of n samples drawn from
975 $\mathcal{N}(\mu, \sigma^2)$. For any $\delta \in (0, 1)$, with probability at least $1 - \delta$, we have*

976
977
$$|\hat{\mu} - \mu| \leq \sigma \sqrt{\frac{2 \ln(2/\delta)}{n}}.$$

978

979 *Proof.* This follows directly from Hoeffding's inequality for sub-Gaussian variables. \square
980981 **Proposition 3** (Random Removal). *Let $p_1, p_2 \in \mathcal{P}$ and $\delta \in (0, 1)$. We observe n_1 samples from p_1
982 and n_2 samples from p_2 , and randomly remove f samples from p_1 before fitting. With probability
983 $1 - \delta$, the resulting MLE distribution satisfies (α, ε) -distributional unlearning with:*

984
985
$$\alpha \geq \left(\frac{1}{2} - 3 \left(\frac{n_1 - f}{n_2} \right)^2 \right) \text{KL}(p_1 \parallel p_2) - \frac{3 \ln(4/\delta)}{2n_2} \left(1 + \frac{n_1 - f}{n_2} \right),$$

986
987
$$\varepsilon \leq 3 \left(\frac{n_1 - f}{n_2} \right)^2 \text{KL}(p_1 \parallel p_2) + \frac{3 \ln(4/\delta)}{n_2} \left(1 + \frac{n_1 - f}{n_2} \right).$$

988
989

990 *Proof.* We recall that $p_1 = \mathcal{N}(\mu_1, \sigma^2), p_2 = \mathcal{N}(\mu_2, \sigma^2) \in \mathcal{P}$ and $p := \mathcal{N}(\mu, \sigma^2) \in \mathcal{P}$ are univariate
991 Gaussian distributions. We are given n_1 i.i.d. samples $x_1^{(1)}, \dots, x_1^{(n_1)}$ from p_1 and n_2 i.i.d. samples
992 $x_2^{(1)}, \dots, x_2^{(n_2)}$ from p_2 .993 Upon removing $f \leq n_1$ randomly chosen samples $x_1^{(1)}, \dots, x_1^{(n_1-f)}$ from the target distribution p_1 ,
994 we set the center μ of the unlearned distribution p to be:
995

996
997
$$\mu = \frac{(n_1 - f)\hat{\mu}_1 + n_2\hat{\mu}_2}{n_1 - f + n_2}, \quad (9)$$

998

999 where $\hat{\mu}_1 := \frac{1}{n_1-f} \sum_{i=1}^{n_1-f} x_1^{(i)}$ and $\hat{\mu}_2 := \frac{1}{n_2} \sum_{i=1}^{n_2} x_2^{(i)}$. We also observe that a standard Hoeffding
1000 bound (Lemma 5) yields that:

1001
1002
$$|\hat{\mu}_1 - \mu_1| \leq \sigma \sqrt{\frac{2 \ln(4/\delta)}{f}}, \quad |\hat{\mu}_2 - \mu_2| \leq \sigma \sqrt{\frac{2 \ln(4/\delta)}{n_2}}, \quad (10)$$

1003
1004

1005 each with probability $1 - \frac{\delta}{2}$, so that both hold with probability $1 - \delta$ thanks to a union bound. We
1006 also recall that

1007
1008
$$\text{KL}(p_1 \parallel p) = \frac{(\mu_1 - \mu)^2}{2\sigma^2}, \quad \text{KL}(p_2 \parallel p) = \frac{(\mu_2 - \mu)^2}{2\sigma^2}. \quad (11)$$

1009 **Preservation bound.** First, we upper bound the KL divergence of p_2 from p . To do so, we first
1010 use the triangle inequality to get

1011
1012
$$|\mu - \mu_2| = \left| \frac{(n_1 - f)\hat{\mu}_1 + n_2\hat{\mu}_2}{n_1 - f + n_2} - \mu_2 \right| = \left| \frac{n_1 - f}{n_1 - f + n_2}(\hat{\mu}_1 - \mu_2) + \frac{n_2}{n_1 - f + n_2}(\hat{\mu}_2 - \mu_2) \right|$$

1013
1014
$$= \left| \frac{n_1 - f}{n_1 - f + n_2}(\mu_1 - \mu_2) + \frac{n_1 - f}{n_1 - f + n_2}(\hat{\mu}_1 - \mu_1) + \frac{n_2}{n_1 - f + n_2}(\hat{\mu}_2 - \mu_2) \right|$$

1015
1016
$$\leq \frac{n_1 - f}{n_1 - f + n_2} |\mu_1 - \mu_2| + \frac{n_1 - f}{n_1 - f + n_2} |\hat{\mu}_1 - \mu_1| + \frac{n_2}{n_1 - f + n_2} |\hat{\mu}_2 - \mu_2|.$$

1017
1018

1019 Therefore, using (10) we have with probability $1 - \delta$:

1020
1021
$$|\mu - \mu_2| \leq \frac{n_1 - f}{n_1 - f + n_2} |\mu_1 - \mu_2| + \frac{n_1 - f}{n_1 - f + n_2} \sigma \sqrt{\frac{2 \ln(4/\delta)}{f}} + \frac{n_2}{n_1 - f + n_2} \sigma \sqrt{\frac{2 \ln(4/\delta)}{n_2}}.$$

1022

1023 Taking squares, using Jensen's inequality, and simplifying further since $f \geq 0$, yields:

1024
1025
$$|\mu - \mu_2|^2 \leq 3 \left(\frac{n_1 - f}{n_2} \right)^2 |\mu_1 - \mu_2|^2 + 3 \left(\frac{n_1 - f}{n_2} \right)^2 \sigma^2 \frac{2 \ln(4/\delta)}{n_1 - f} + \sigma^2 \frac{6 \ln(4/\delta)}{n_2}. \quad (12)$$

1026 Dividing both sides by $2\sigma^2$ and then using (28) yields with probability $1 - \delta$:
 1027

$$1028 \text{KL}(p_2 \parallel p) \leq 3 \left(\frac{n_1 - f}{n_2} \right)^2 \text{KL}(p_1 \parallel p_2) + \frac{3 \ln(4/\delta)}{n_2} \left(1 + \frac{n_1 - f}{n_2} \right). \quad (13)$$

1029
1030

1031 **Removal bound.** Second, we lower bound the KL divergence of p_1 from p . To do so, we use
 1032 Jensen's inequality and (12) to obtain that, with probability $1 - \delta$, we have
 1033

$$1034 |\mu_1 - \mu_2|^2 = |\mu_1 - \mu + \mu - \mu_2|^2 \leq 2|\mu_1 - \mu|^2 + 2|\mu - \mu_2|^2$$

$$1035 \leq 2|\mu_1 - \mu|^2 + 6 \left(\frac{n_1 - f}{n_2} \right)^2 |\mu_1 - \mu_2|^2 + \frac{6\sigma^2 \ln(4/\delta)}{n_2} \left(1 + \frac{n_1 - f}{n_2} \right)$$

1036
1037

1038 Rearranging terms and dividing by $4\sigma^2$ along with (28) yields that with probability $1 - \delta$ we have
 1039

$$1040 \text{KL}(p_1 \parallel p) = \frac{|\mu_1 - \mu|^2}{2\sigma^2} \geq \frac{|\mu_1 - \mu_2|^2}{4\sigma^2} - 3 \left(\frac{n_1 - f}{n_2} \right)^2 \frac{|\mu_1 - \mu_2|^2}{2\sigma^2} - \frac{3 \ln(4/\delta)}{2n_2} \left(1 + \frac{n_1 - f}{n_2} \right)$$

$$1041 = \left(\frac{1}{2} - 3 \left(\frac{n_1 - f}{n_2} \right)^2 \right) \text{KL}(p_1 \parallel p_2) - \frac{3 \ln(4/\delta)}{2n_2} \left(1 + \frac{n_1 - f}{n_2} \right).$$

1042
1043
1044

1045 **Conclusion.** With probability $1 - \delta$, we have (α, ε) -distributional unlearning with
 1046

$$1047 \alpha \geq \left(\frac{1}{2} - 3 \left(\frac{n_1 - f}{n_2} \right)^2 \right) \text{KL}(p_1 \parallel p_2) - \frac{3 \ln(4/\delta)}{2n_2} \left(1 + \frac{n_1 - f}{n_2} \right),$$

$$1048 \varepsilon \leq 3 \left(\frac{n_1 - f}{n_2} \right)^2 \text{KL}(p_1 \parallel p_2) + \frac{3 \ln(4/\delta)}{n_2} \left(1 + \frac{n_1 - f}{n_2} \right).$$

1049
1050
1051
1052

□

1055 A.4 SELECTIVE REMOVAL

1056

1057 **Lemma 6** (Dvoretzky–Kiefer–Wolfowitz Inequality). *Let x_1, x_2, \dots, x_n be independent and iden-
 1058 tically distributed random variables with cumulative distribution function F . Define the empirical
 1059 distribution function by*

$$1060 \hat{F}(t) = \frac{1}{n} \sum_{i=1}^n \mathbb{1}\{x_i \leq t\}.$$

1061
1062

1063 Then, for any $\delta \in (0, 1)$, with probability at least $1 - \delta$ we have

$$1064 \sup_{t \in \mathbb{R}} |\hat{F}(t) - F(t)| \leq \sqrt{\frac{\ln(2/\delta)}{2n}}.$$

1065
1066

1067 **Lemma 7.** *Let $\mu_1, \mu_2 \in \mathbb{R}$, $\sigma > 0$. Consider n_1 i.i.d. samples $x_1^{(1)}, \dots, x_1^{(n_1)}$ from $\mathcal{N}(\mu_1, \sigma^2)$ and
 1068 n_2 i.i.d. samples $x_2^{(1)}, \dots, x_2^{(n_2)}$ from $\mathcal{N}(\mu_2, \sigma^2)$. We define $\hat{\mu}_2$ the average of the samples from
 1069 $\mathcal{N}(\mu_2, \sigma^2)$, $\hat{\mu}_1$ the average of the $n_1 - f \leq n_1$ closest samples from $x_1^{(1)}, \dots, x_1^{(n_1)}$ to $\hat{\mu}_2$. We define
 1070 $F : t \in \mathbb{R} \mapsto \Phi(\frac{t - |\mu_1 - \mu_2|}{\sigma}) - \Phi(\frac{-t - |\mu_1 - \mu_2|}{\sigma})$, where Φ is the standard normal CDF.
 1071*

1072 For any $\delta \in (0, 1)$, we have with probability $1 - \delta$,

$$1073 |\hat{\mu}_1 - \mu_2| \leq F^{-1} \left(1 - \frac{f}{n_1} + \sqrt{\frac{\ln(2/\delta)}{2n_1}} \right). \quad (14)$$

1074
1075
1076
1077

1078 *Proof.* Recall from Equation (25) that $\hat{\mu}_1$ is the average of the $n_1 - f$ samples, out of n_1 i.i.d. from
 1079 p_1 , with the closest distance to $\hat{\mu}_2$, the empirical mean of n_2 samples from p_2 .

1080 Denote by $\hat{\tau}_f := |x_1^{(n_1-f:n_1)} - \hat{\mu}_2|$ the $(n_1 - f)$ -th largest distance of $\hat{\mu}_2$ to p_1 samples. It is then
 1081 immediate from the triangle inequality that
 1082

$$1083 |\hat{\mu}_1 - \mu_2| = \left| \frac{1}{n_1 - f} \sum_{i=1}^{n_1-f} x_1^{(i:n_1)} - \mu_2 \right| \leq \frac{1}{n_1 - f} \sum_{i=1}^{n_1-f} |x_1^{(i:n_1)} - \mu_2| \leq \hat{\tau}_f. \quad (15)$$

1086 Besides, denoting by \hat{F}_1 the empirical CDF of the empirical distribution over
 1087 $\{ |x_1^{(i)} - \mu_2| : i \in [n_1] \}$, we have for all $t \in \mathbb{R}$:
 1089

$$1090 \hat{F}_1(t) = \frac{1}{n_1} \sum_{i=1}^{n_1} \mathbb{1}_{\{ |x_1^{(i)} - \mu_2| \leq t \}}. \quad (16)$$

1093 Yet, we recall that with probability $1 - \frac{\delta}{2}$, we have
 1094

$$1095 |\hat{\mu}_2 - \mu_2| \leq \sigma \sqrt{\frac{2 \ln(4/\delta)}{n_2}}. \quad (17)$$

1098 Therefore, the triangle inequality gives for $i \in [n_1]$, $|x_1^{(i)} - \mu_2| \leq |x_1^{(i)} - \hat{\mu}_2| + |\hat{\mu}_2 - \mu_2| \leq$
 1099 $|x_1^{(i)} - \hat{\mu}_2| + \sigma \sqrt{\frac{2 \ln(4/\delta)}{n_2}}$, and we deduce
 1100

$$1102 \hat{F}_1(t) = \frac{1}{n_1} \sum_{i=1}^{n_1} \mathbb{1}_{\{ |x_1^{(i)} - \mu_2| \leq t \}} \leq \frac{1}{n_1} \sum_{i=1}^{n_1} \mathbb{1}_{\{ |x_1^{(i)} - \hat{\mu}_2| \leq t - \sigma \sqrt{\frac{2 \ln(4/\delta)}{n_2}} \}}. \quad (18)$$

1105 In particular, by definition of $\hat{\tau}_f$, we have
 1106

$$1107 \hat{F}_1(\hat{\tau}_f + \sigma \sqrt{\frac{2 \ln(4/\delta)}{n_2}}) \leq \frac{1}{n_1} \sum_{i=1}^{n_1} \mathbb{1}_{\{ |x_1^{(i)} - \hat{\mu}_2| \leq \hat{\tau}_f \}} = \frac{n_1 - f}{n_1} = 1 - \frac{f}{n_1}. \quad (19)$$

1110 Now, observe that $|x_1^{(i)} - \mu_2|$ follows a folded normal distribution of location $\mu_1 - \mu_2$ and
 1111 scale σ^2 , since $x_1^{(i)}$ follows $p_1 = \mathcal{N}(\mu_1, \sigma^2)$. Denote by F_1 its CDF. Thanks to the Dvoretzky–Kiefer–Wolfowitz inequality (Lemma 6), we have with probability $1 - \frac{\delta}{2}$ that for all $t \in \mathbb{R}$,
 1113

$$1114 |\hat{F}_1(t) - F_1(t)| \leq \sqrt{\frac{\ln(4/\delta)}{2n_1}}. \quad (20)$$

1117 Plugging the above in the previous inequality, and using a union bound, we get with probability
 1118 $1 - \delta$,
 1119

$$1120 F_1(\hat{\tau}_f + \sigma \sqrt{\frac{2 \ln(4/\delta)}{n_2}}) \leq \hat{F}_1(\hat{\tau}_f + \sigma \sqrt{\frac{2 \ln(4/\delta)}{n_2}}) + \sqrt{\frac{\ln(4/\delta)}{2n_1}} \leq 1 - \frac{f}{n_1} + \sqrt{\frac{\ln(4/\delta)}{2n_1}}. \quad (21)$$

1123 By taking the inverse F_1^{-1} of the CDF F_1 and rearranging terms, we obtain with probability $1 - \delta$
 1124 that

$$1125 \hat{\tau}_f \leq F_1^{-1} \left(1 - \frac{f}{n_1} + \sqrt{\frac{\ln(4/\delta)}{2n_1}} \right) - \sigma \sqrt{\frac{2 \ln(4/\delta)}{n_2}}. \quad (22)$$

1128 Finally, going back to (15), we obtain with probability $1 - \delta$ that
 1129

$$1130 |\hat{\mu}_1 - \mu_2| \leq \hat{\tau}_f \leq F_1^{-1} \left(1 - \frac{f}{n_1} + \sqrt{\frac{\ln(4/\delta)}{2n_1}} \right) - \sigma \sqrt{\frac{2 \ln(4/\delta)}{n_2}}. \quad (23)$$

□

1134 **Lemma 8.** Let $\mu_1, \mu_2 \in \mathbb{R}$ and suppose that $x \sim \mathcal{N}(\mu_1, \sigma^2)$. Define the random variable $z :=$
 1135 $|x - \mu_2|$, with cumulative distribution function
 1136

$$1137 F_\sigma(t) := \mathbb{P}[z \leq t] = \Phi\left(\frac{t - |\mu_1 - \mu_2|}{\sigma}\right) - \Phi\left(\frac{-t - |\mu_1 - \mu_2|}{\sigma}\right), \quad t \geq 0,$$

1139 where Φ denotes the standard normal CDF. Then, for any $p \in (0, 1)$ the inverse CDF satisfies
 1140

$$1141 F_\sigma^{-1}(p) = \sigma g^{-1}\left(p; \frac{|\mu_1 - \mu_2|^2}{2\sigma^2}\right),$$

1143 where the function $g(u; \kappa)$ is defined by $g(u; \kappa) := \Phi(u - \sqrt{2\kappa}) + \Phi(u + \sqrt{2\kappa}) - 1$, and $g^{-1}(p; \kappa)$
 1144 denotes the inverse function in u satisfying $g(u; \kappa) = p$. In particular, when $\mu_1 = \mu_2$ (so that $\kappa = 0$)
 1145 we have $g(u; 0) = 2\Phi(u) - 1$ and thus $F_{0,1}^{-1}(p) = \Phi^{-1}\left(\frac{p+1}{2}\right)$.
 1146

1147 *Proof.* Since $x \sim \mathcal{N}(\mu_1, \sigma^2)$, we have that $z = |x - \mu_2|$ has CDF
 1148

$$1149 F_\sigma(t) = \Phi\left(\frac{t - |\mu_1 - \mu_2|}{\sigma}\right) - \Phi\left(\frac{-t - |\mu_1 - \mu_2|}{\sigma}\right), \quad t \geq 0.$$

1150 Introduce the change of variable $u = \frac{t}{\sigma}$ so that $t = \sigma u$. Then,
 1151

$$1152 F_\sigma(\sigma u) = \Phi\left(u - \frac{|\mu_1 - \mu_2|}{\sigma}\right) - \Phi\left(-u - \frac{|\mu_1 - \mu_2|}{\sigma}\right).$$

1153 Using the symmetry $\Phi(-x) = 1 - \Phi(x)$, this becomes
 1154

$$1155 F_\sigma(\sigma u) = \Phi\left(u - \frac{|\mu_1 - \mu_2|}{\sigma}\right) + \Phi\left(u + \frac{|\mu_1 - \mu_2|}{\sigma}\right) - 1.$$

1156 Defining $\kappa = \frac{|\mu_1 - \mu_2|^2}{2\sigma^2}$ and setting
 1157

$$1158 g(u; \kappa) := \Phi(u - \sqrt{2\kappa}) + \Phi(u + \sqrt{2\kappa}) - 1,$$

1159 we have $F_\sigma(\sigma u) = g(u; \kappa)$. Thus, if u^* is the unique solution of $g(u^*; \kappa) = p$, then
 1160

$$1161 F_\sigma(\sigma u^*) = p,$$

1162 so that
 1163

$$1164 F_\sigma^{-1}(p) = \sigma u^* = \sigma g^{-1}(p; \kappa).$$

1165 In the special case $\mu_1 = \mu_2$ (so that $\kappa = 0$), we obtain $g(u; 0) = 2\Phi(u) - 1$, whose inverse is given
 1166 by $u = \Phi^{-1}((p+1)/2)$. Hence, $F_1^{-1}(p) = \Phi^{-1}((p+1)/2)$, as required. \square
 1167

1168 **Theorem 1** (Selective Removal). Let $p_1, p_2 \in \mathcal{P}$ and $\delta \in (0, 1)$. Let f samples from p_1 be re-
 1169 moved according to Selective Removal. With probability $1 - \delta$, the resulting estimate satisfies
 1170 (α, ε) -distributional unlearning with:
 1171

$$1172 \alpha \geq \frac{1}{2} \text{KL}(p_1 \parallel p_2) - \frac{1}{2} \left(\frac{n_1 - f}{n_2}\right)^2 g^{-1}\left(1 - \frac{f}{n_1} + \sqrt{\frac{\ln(4/\delta)}{2n_1}}; \text{KL}(p_1 \parallel p_2)\right)^2 - \frac{\ln(4/\delta)}{n_2},$$

$$1173 \varepsilon \leq \left(\frac{n_1 - f}{n_2}\right)^2 g^{-1}\left(1 - \frac{f}{n_1} + \sqrt{\frac{\ln(4/\delta)}{2n_1}}; \text{KL}(p_1 \parallel p_2)\right)^2 + \frac{2\ln(4/\delta)}{n_2},$$

1174 where $g(u; \kappa) := \Phi(u - \sqrt{2\kappa}) + \Phi(u + \sqrt{2\kappa}) - 1$, for $u, \kappa > 0$, and Φ is the standard normal CDF.
 1175

1176 *Proof.* We recall that $p_1 = \mathcal{N}(\mu_1, \sigma^2), p_2 = \mathcal{N}(\mu_2, \sigma^2) \in \mathcal{P}$ and $p := \mathcal{N}(\mu, \sigma^2) \in \mathcal{P}$ are univariate
 1177 Gaussian distributions. We are given n_1 i.i.d. samples $x_1^{(1)}, \dots, x_1^{(n_1)}$ from p_1 and n_2 i.i.d. samples
 1178 $x_2^{(1)}, \dots, x_2^{(n_2)}$ from p_2 .
 1179

1180 The distance-based selection removes $f \leq n_1$ selected samples from the target distribution p_1 with
 1181 the f largest distances to $\hat{\mu}_2 := \frac{1}{n_2} \sum_{i=1}^{n_2} x_2^{(i)}$ the empirical estimator of the mean of p_2 . That is,
 1182

denoting by $x_1^{(1:n_1)}, \dots, x_1^{(n_1:n_1)}$ the original n_1 samples from p_1 reordered by increasing distance to $\hat{\mu}_2$:

$$|x_1^{(1:n_1)} - \hat{\mu}_2| \leq \dots \leq |x_1^{(n_1:n_1)} - \hat{\mu}_2|, \quad (24)$$

with ties broken arbitrarily, then distance-based selection retains only $x_1^{(1:n_1)}, \dots, x_1^{(n_1-f:n_1)}$ to obtain

$$\hat{\mu}_1 := \frac{1}{n_1-f} \sum_{i=1}^{n_1-f} x_1^{(i:n_1)}. \quad (25)$$

Subsequently, we set the center μ of the unlearned distribution p to be:

$$\mu = \frac{(n_1-f)\hat{\mu}_1 + n_2\hat{\mu}_2}{n_1-f+n_2}, \quad (26)$$

where $\hat{\mu}_1 = \frac{1}{n_1-f} \sum_{i=1}^{n_1-f} x_1^{(i:n_1)}$ and $\hat{\mu}_2 = \frac{1}{n_2} \sum_{i=1}^{n_2} x_2^{(i)}$. We also observe that a standard Hoeffding bound (Lemma 5) yields that:

$$|\hat{\mu}_2 - \mu_2| \leq \sigma \sqrt{\frac{2 \ln(4/\delta)}{n_2}}, \quad (27)$$

with probability $1 - \frac{\delta}{2}$. We also recall that

$$\text{KL}(p_1 \parallel p) = \frac{(\mu_1 - \mu)^2}{2\sigma^2}, \quad \text{KL}(p_2 \parallel p) = \frac{(\mu_2 - \mu)^2}{2\sigma^2}. \quad (28)$$

Preservation bound. First, we upper bound the KL divergence of p_2 from p . To do so, we first use the triangle inequality to get

$$\begin{aligned} |\mu - \mu_2| &= \left| \frac{(n_1-f)\hat{\mu}_1 + n_2\hat{\mu}_2}{n_1-f+n_2} - \mu_2 \right| = \left| \frac{n_1-f}{n_1-f+n_2}(\hat{\mu}_1 - \mu_2) + \frac{n_2}{n_1-f+n_2}(\hat{\mu}_2 - \mu_2) \right| \\ &\leq \frac{n_1-f}{n_1-f+n_2} |\hat{\mu}_1 - \mu_2| + \frac{n_2}{n_1-f+n_2} |\hat{\mu}_2 - \mu_2|. \end{aligned}$$

Therefore, using (27) we have with probability $1 - \frac{\delta}{2}$:

$$|\mu - \mu_2| \leq \frac{n_1-f}{n_1-f+n_2} |\hat{\mu}_1 - \mu_2| + \frac{n_2}{n_1-f+n_2} \sigma \sqrt{\frac{2 \ln(4/\delta)}{n_2}}.$$

Moreover, we know from Lemma 7 that with probability $1 - \frac{\delta}{2}$

$$|\hat{\mu}_1 - \mu_2| \leq F^{-1} \left(1 - \frac{f}{n_1} + \sqrt{\frac{\ln(4/\delta)}{2n_1}} \right).$$

Using the above in the previous inequality with a union bound, yields that with probability $1 - \delta$

$$|\mu - \mu_2| \leq \frac{n_1-f}{n_1-f+n_2} F^{-1} \left(1 - \frac{f}{n_1} + \sqrt{\frac{\ln(4/\delta)}{2n_1}} \right) + \frac{n_2}{n_1-f+n_2} \sigma \sqrt{\frac{2 \ln(4/\delta)}{n_2}}.$$

We can further simplify the above using Lemma 8, which implies that for all $p > 0$

$$F^{-1}(p) = \sigma g^{-1} \left(p; \frac{|\mu_1 - \mu_2|^2}{2\sigma^2} \right),$$

where the function g is defined by $g(u; \kappa) := \Phi(u - \sqrt{2\kappa}) + \Phi(u + \sqrt{2\kappa}) - 1$, for $u, \kappa > 0$. Plugging this in the previous bound yields

$$|\mu - \mu_2| \leq \frac{n_1-f}{n_1-f+n_2} \sigma g^{-1} \left(1 - \frac{f}{n_1} + \sqrt{\frac{\ln(4/\delta)}{2n_1}}; \frac{|\mu_1 - \mu_2|^2}{2\sigma^2} \right) + \frac{n_2}{n_1-f+n_2} \sigma \sqrt{\frac{2 \ln(4/\delta)}{n_2}}. \quad (29)$$

Dividing both sides by $\sigma\sqrt{2}$ and then using (28) yields with probability $1 - \delta$:

$$\sqrt{\text{KL}(p_2 \parallel p)} \leq \frac{n_1 - f}{(n_1 - f + n_2)\sqrt{2}} g^{-1} \left(1 - \frac{f}{n_1} + \sqrt{\frac{\ln(4/\delta)}{2n_1}}; \text{KL}(p_1 \parallel p_2) \right) + \frac{\sqrt{n_2 \log(4/\delta)}}{n_1 - f + n_2}. \quad (30)$$

The above directly implies, by taking squares and using Jensen's inequality and that $f \geq 0$, that with probability $1 - \delta$:

$$\text{KL}(p_2 \parallel p) \leq \left(\frac{n_1 - f}{n_2} \right)^2 g^{-1} \left(1 - \frac{f}{n_1} + \sqrt{\frac{\ln(4/\delta)}{2n_1}}; \text{KL}(p_1 \parallel p_2) \right)^2 + \frac{2 \ln(4/\delta)}{n_2}. \quad (31)$$

Removal bound. Second, we lower bound the KL divergence of p_1 from p . To do so, we use Jensen's inequality and (29) to obtain that, with probability $1 - \delta$, we have

$$\begin{aligned} |\mu_1 - \mu_2|^2 &= |\mu_1 - \mu + \mu - \mu_2|^2 \leq 2|\mu_1 - \mu|^2 + 2|\mu - \mu_2|^2 \\ &\leq 2|\mu_1 - \mu|^2 + 2 \left(\frac{n_1 - f}{n_1 - f + n_2} \right)^2 \sigma^2 g^{-1} \left(1 - \frac{f}{n_1} + \sqrt{\frac{\ln(4/\delta)}{2n_1}}; \frac{|\mu_1 - \mu_2|^2}{2\sigma^2} \right)^2 \\ &\quad + \left(\frac{n_2}{n_1 - f + n_2} \right)^2 \sigma^2 \frac{4 \ln(4/\delta)}{n_2}. \end{aligned}$$

Rearranging terms, using that $f \geq 0$, and dividing by $4\sigma^2$ along with (28) yields that with probability $1 - \delta$ we have

$$\begin{aligned} \text{KL}(p_1 \parallel p) &= \frac{|\mu_1 - \mu|^2}{2\sigma^2} \geq \frac{|\mu_1 - \mu_2|^2}{4\sigma^2} - \frac{1}{2} \left(\frac{n_1 - f}{n_2} \right)^2 g^{-1} \left(1 - \frac{f}{n_1} + \sqrt{\frac{\ln(4/\delta)}{2n_1}}; \frac{|\mu_1 - \mu_2|^2}{2\sigma^2} \right)^2 - \frac{\ln(4/\delta)}{n_2} \\ &= \frac{1}{2} \text{KL}(p_1 \parallel p_2) - \frac{1}{2} \left(\frac{n_1 - f}{n_2} \right)^2 g^{-1} \left(1 - \frac{f}{n_1} + \sqrt{\frac{\ln(4/\delta)}{2n_1}}; \frac{|\mu_1 - \mu_2|^2}{2\sigma^2} \right)^2 - \frac{\ln(4/\delta)}{n_2}. \end{aligned}$$

Now, using (28) we get

$$\text{KL}(p_1 \parallel p) \geq \frac{1}{2} \text{KL}(p_1 \parallel p_2) - \frac{1}{2} \left(\frac{n_1 - f}{n_2} \right)^2 g^{-1} \left(1 - \frac{f}{n_1} + \sqrt{\frac{\ln(4/\delta)}{2n_1}}; \text{KL}(p_1 \parallel p_2) \right)^2 - \frac{\ln(4/\delta)}{n_2}$$

Conclusion. With probability $1 - \delta$, we have (α, ε) -distributional unlearning with

$$\begin{aligned} \alpha &\geq \frac{1}{2} \text{KL}(p_1 \parallel p_2) - \frac{1}{2} \left(\frac{n_1 - f}{n_2} \right)^2 g^{-1} \left(1 - \frac{f}{n_1} + \sqrt{\frac{\ln(4/\delta)}{2n_1}}; \text{KL}(p_1 \parallel p_2) \right)^2 - \frac{\ln(4/\delta)}{n_2}, \\ \varepsilon &\leq \left(\frac{n_1 - f}{n_2} \right)^2 g^{-1} \left(1 - \frac{f}{n_1} + \sqrt{\frac{\ln(4/\delta)}{2n_1}}; \text{KL}(p_1 \parallel p_2) \right)^2 + \frac{2 \ln(4/\delta)}{n_2}. \end{aligned}$$

□

A.5 SIMPLIFIED SAMPLE COMPLEXITY FOR SELECTIVE REMOVAL

In this section, we can simplify the result of Theorem 1 on selective removal by simplifying cumbersome terms. This leads to Corollary 10, which then yields to the sample complexity results in Table 1.

We first prove an upper bound on the inverse CDF of a folded Normal for small quantiles.

Lemma 9. Let $\mu_1, \mu_2 \in \mathbb{R}$, $\sigma > 0$, and $x \sim \mathcal{N}(\mu_1, \sigma^2)$. Define the random variable $z = |x - \mu_2|$, which follows a folded normal distribution whose cumulative distribution function (CDF) is given by

$$F(t) := \mathbb{P}[z \leq t] = \Phi \left(\frac{t - |\mu_1 - \mu_2|}{\sigma} \right) - \Phi \left(\frac{-t - |\mu_1 - \mu_2|}{\sigma} \right), \quad t \geq 0, \quad (32)$$

1296 where Φ denotes the standard normal CDF. Then, for any $p > 0$ such that $F^{-1}(p) \leq |\mu_1 - \mu_2|$, it
 1297 holds that:

$$1298 \quad 1299 \quad 1300 \quad F^{-1}(p) \leq \frac{\sigma p}{\varphi\left(\frac{|\mu_1 - \mu_2|}{\sigma}\right)},$$

1301 where $\varphi(x) := \frac{1}{\sqrt{2\pi}} \exp\left(-\frac{x^2}{2}\right)$, $x \in \mathbb{R}$, is the standard normal density.
 1302

1303 *Proof.* Since F , defined in (32), is continuously differentiable and strictly increasing on $[0, |\mu_1 - \mu_2|]$
 1304 (with $F(0) = 0$) and by the assumption $F^{-1}(p) \leq |\mu_1 - \mu_2|$, the Mean Value Theorem guarantees
 1305 that there exists some $\xi \in [0, F^{-1}(p)]$ such that

$$1307 \quad F\left(F^{-1}(p)\right) = F(0) + F'(\xi)\left(F^{-1}(p) - 0\right).$$

1309 Since $F(0) = 0$ and F is strictly increasing, one may directly write, via the Mean Value Theorem,
 1310 that there exists $\xi \in [0, F^{-1}(p)]$ with

$$1311 \quad 1312 \quad F\left(F^{-1}(p)\right) = F'(\xi) F^{-1}(p).$$

1313 By definition of the inverse CDF, $F\left(F^{-1}(p)\right) = p$; hence,

$$1315 \quad 1316 \quad p = F'(\xi) F^{-1}(p).$$

1317 It remains to lower-bound $F'(\xi)$ for $\xi \in [0, |\mu_1 - \mu_2|]$. We recall that for $t \geq 0$,

$$1319 \quad 1320 \quad F(t) = \Phi\left(\frac{t - |\mu_1 - \mu_2|}{\sigma}\right) - \Phi\left(\frac{-t - |\mu_1 - \mu_2|}{\sigma}\right).$$

1321 Taking the derivative with respect to t yields

$$1322 \quad 1323 \quad 1324 \quad 1325 \quad 1326 \quad F'(t) = \frac{1}{\sigma} \varphi\left(\frac{t - |\mu_1 - \mu_2|}{\sigma}\right) + \frac{1}{\sigma} \varphi\left(\frac{-t - |\mu_1 - \mu_2|}{\sigma}\right) \\ = \frac{1}{\sigma} \varphi\left(\frac{t - |\mu_1 - \mu_2|}{\sigma}\right) + \frac{1}{\sigma} \varphi\left(\frac{t + |\mu_1 - \mu_2|}{\sigma}\right),$$

1327 where we used that the standard normal density ϕ is symmetric.

1328 For $t \in [0, |\mu_1 - \mu_2|]$, observe that $t - |\mu_1 - \mu_2| \leq 0$. Because the standard normal density is
 1329 symmetric and nonincreasing on $[0, \infty)$, we have

$$1331 \quad 1332 \quad \varphi\left(\frac{t - |\mu_1 - \mu_2|}{\sigma}\right) = \varphi\left(\frac{|\mu_1 - \mu_2| - t}{\sigma}\right) \geq \varphi\left(\frac{|\mu_1 - \mu_2|}{\sigma}\right).$$

1333 Also, the second term $\varphi\left(\frac{t + |\mu_1 - \mu_2|}{\sigma}\right)$ is nonnegative. Hence, for all $t \in [0, |\mu_1 - \mu_2|]$ we have

$$1335 \quad 1336 \quad F'(t) \geq \frac{1}{\sigma} \varphi\left(\frac{|\mu_1 - \mu_2|}{\sigma}\right).$$

1337 In particular, at $t = \xi$ we obtain

$$1339 \quad 1340 \quad F'(\xi) \geq \frac{1}{\sigma} \varphi\left(\frac{|\mu_1 - \mu_2|}{\sigma}\right).$$

1341 Substituting this lower bound into the equation $p = F'(\xi) F^{-1}(p)$ yields

$$1343 \quad 1344 \quad p \geq \frac{F^{-1}(p)}{\sigma} \varphi\left(\frac{|\mu_1 - \mu_2|}{\sigma}\right).$$

1345 Rearranging the inequality gives the desired upper bound:

$$1347 \quad 1348 \quad 1349 \quad F^{-1}(p) \leq \frac{\sigma p}{\varphi\left(\frac{|\mu_1 - \mu_2|}{\sigma}\right)}.$$

1349 This completes the proof. \square

We are now ready to prove the corollary below. Note that retaining dependences on α, ε only in this corollary leads to the result of Table 1.

Corollary 10. *Let $p_1, p_2 \in \mathcal{P}$ and $\delta \in (0, 1)$. Let f samples from p_1 be removed according to our distance-based scoring rule or at random before MLE. Then in each case, with probability at least $1 - \delta$, the resulting estimate satisfies (α, ε) -distributional unlearning if:*

1. *Random removal: $n_2 \geq \frac{12 \ln(4/\delta)}{\min\{\varepsilon, \alpha\}}$ and $\text{KL}(p_1 \parallel p_2) \geq 8\alpha$, and*

$$f \geq n_1 - n_2 \sqrt{\frac{2\text{KL}(p_1 \parallel p_2) - \alpha}{12\text{KL}(p_1 \parallel p_2)}}, \quad f \geq n_1 - n_2 \min\left\{1, \sqrt{\frac{\varepsilon}{6\text{KL}(p_1 \parallel p_2)}}\right\}.$$

2. *Selective removal: $n_2 \geq 2 \ln(4/\delta) \max\left\{\frac{1}{\varepsilon}, \frac{1}{\sqrt{\varepsilon}}, \frac{1}{\alpha}, \sqrt{\text{KL}(p_1 \parallel p_2) - 4\alpha}\right\}$, $\text{KL}(p_1 \parallel p_2) \geq 4\alpha$, and $f \geq n_1 \left(\frac{3}{2} + \sqrt{\frac{\ln(4/\delta)}{2n_1}} - \Phi(2\sqrt{2\text{KL}(p_1 \parallel p_2)})\right)$, and*

$$f \geq n_1 - \sqrt{n_1 n_2} \left(\frac{\varepsilon}{16\pi}\right)^{1/4} \exp(-\text{KL}(p_1 \parallel p_2)),$$

$$f \geq n_1 - \sqrt{n_1 n_2} \left(\frac{\text{KL}(p_1 \parallel p_2) - 4\alpha}{8\pi}\right)^{1/4} \exp(-\text{KL}(p_1 \parallel p_2)).$$

Proof. We treat random and selective removal separately below.

Random Removal. Consider removing f samples using the random removal mechanism, before maximum likelihood estimation. From Theorem 3, with probability $1 - \delta$, we achieve (α, ε) -unlearning with:

$$\alpha \geq \left(\frac{1}{2} - 3 \left(\frac{n_1 - f}{n_2}\right)^2\right) \text{KL}(p_1 \parallel p_2) - \frac{3 \ln(4/\delta)}{2n_2} \left(1 + \frac{n_1 - f}{n_2}\right) \quad (\text{removal}),$$

$$\varepsilon \leq 3 \left(\frac{n_1 - f}{n_2}\right)^2 \text{KL}(p_1 \parallel p_2) + \frac{3 \ln(4/\delta)}{n_2} \left(1 + \frac{n_1 - f}{n_2}\right) \quad (\text{preservation}).$$

Therefore, assuming that $n_2 \geq \frac{12 \ln(4/\delta)}{\min\{\varepsilon, \alpha\}}$ and $\text{KL}(p_1 \parallel p_2) \geq 8\alpha$, direct calculations show that it is sufficient to set:

$$f \geq n_1 - n_2 \sqrt{\frac{2\text{KL}(p_1 \parallel p_2) - \alpha}{12\text{KL}(p_1 \parallel p_2)}} \quad (\text{removal}),$$

$$f \geq n_1 - n_2 \min\left\{1, \sqrt{\frac{\varepsilon}{6\text{KL}(p_1 \parallel p_2)}}\right\} \quad (\text{preservation}).$$

Selective Removal. For selective removal, Theorem 1 shows that, with probability $1 - \delta$, we achieve (α, ε) -unlearning with:

$$\alpha \geq \frac{1}{2} \text{KL}(p_1 \parallel p_2) - \frac{1}{2} \left(\frac{n_1 - f}{n_2}\right)^2 g^{-1}\left(1 - \frac{f}{n_1} + \sqrt{\frac{\ln(4/\delta)}{2n_1}}; \text{KL}(p_1 \parallel p_2)\right)^2 - \frac{\ln(4/\delta)}{n_2} \quad (\text{removal}),$$

$$\varepsilon \leq \left(\frac{n_1 - f}{n_2}\right)^2 g^{-1}\left(1 - \frac{f}{n_1} + \sqrt{\frac{\ln(4/\delta)}{2n_1}}; \text{KL}(p_1 \parallel p_2)\right)^2 + \frac{2 \ln(4/\delta)}{n_2} \quad (\text{preservation}).$$

We can simplify these bounds using Lemma 9. Indeed, thanks to the latter and using the same notation and a simple change of variable, we have for all $p, \kappa > 0$ such that $p \leq F(|\mu_1 - \mu_2|)$

$$g^{-1}(p; \kappa) \leq \frac{p}{\phi(\sqrt{2\kappa})} = p\sqrt{2\pi} \exp(\kappa). \quad (33)$$

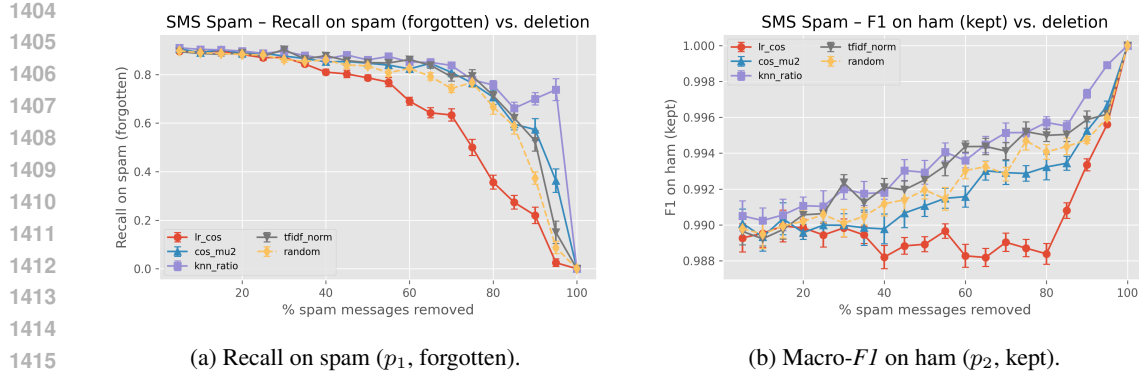


Figure 5: **SMS Spam.** The likelihood-ratio score (LR-COS) pushes spam recall below 0.6 after deleting 70% of spam, whereas random deletion needs nearly 90% removal to reach the same point. Ham performance remains almost flat (<0.004 absolute change) until the final 100 % budget, affirming the tight preservation guarantee. Error bars: ± 1 standard error over ten seeds.

Now, we plug in $p = 1 - \frac{f}{n_1} + \sqrt{\frac{\ln(4/\delta)}{2n_1}}$. Assuming $f \geq n_1 \left(-\Phi(2\sqrt{2\text{KL}(p_1 \parallel p_2)}) + \frac{3}{2} + \sqrt{\frac{\ln(4/\delta)}{2n_1}} \right)$, which directly implies that $p \leq F(|\mu_1 - \mu_2|)$ as required, we then obtain

$$g^{-1} \left(1 - \frac{f}{n_1} + \sqrt{\frac{\ln(4/\delta)}{2n_1}}; \text{KL}(p_1 \parallel p_2) \right) \leq \left(1 - \frac{f}{n_1} + \sqrt{\frac{\ln(4/\delta)}{2n_1}} \right) \sqrt{2\pi} \exp(\text{KL}(p_1 \parallel p_2)).$$

Plugging the above back in the first bounds due to Theorem 1, we obtain:

$$\begin{aligned} \alpha &\geq \frac{1}{2} \text{KL}(p_1 \parallel p_2) - \frac{1}{2} \left(\frac{n_1 - f}{n_2} \right)^2 \left(1 - \frac{f}{n_1} + \sqrt{\frac{\ln(4/\delta)}{2n_1}} \right)^2 2\pi \exp(2\text{KL}(p_1 \parallel p_2)) - \frac{\ln(4/\delta)}{n_2}, \\ \varepsilon &\leq \left(\frac{n_1 - f}{n_2} \right)^2 \left(1 - \frac{f}{n_1} + \sqrt{\frac{\ln(4/\delta)}{2n_1}} \right)^2 2\pi \exp(2\text{KL}(p_1 \parallel p_2)) + \frac{2\ln(4/\delta)}{n_2}. \end{aligned}$$

Therefore, assuming that $n_2 \geq 2\ln(4/\delta) \max \left\{ \frac{1}{\varepsilon}, \frac{1}{\sqrt{\varepsilon}}, \frac{1}{\alpha}, \sqrt{\text{KL}(p_1 \parallel p_2) - 4\alpha} \right\}$ and $\text{KL}(p_1 \parallel p_2) \geq 4\alpha$, and recalling we had assumed $f \geq n_1 \left(-\Phi(2\sqrt{2\text{KL}(p_1 \parallel p_2)}) + \frac{3}{2} + \sqrt{\frac{\ln(4/\delta)}{2n_1}} \right)$, direct calculations show that it is sufficient to set:

$$f \geq n_1 - \sqrt{n_1 n_2} \left(\frac{\varepsilon}{16\pi} \right)^{1/4} \exp(-\text{KL}(p_1 \parallel p_2)) \quad (\text{removal}),$$

$$f \geq n_1 - \sqrt{n_1 n_2} \left(\frac{\text{KL}(p_1 \parallel p_2) - 4\alpha}{8\pi} \right)^{1/4} \exp(-\text{KL}(p_1 \parallel p_2)) \quad (\text{preservation}).$$

□

B EXPERIMENTAL DETAILS AND ADDITIONAL RESULTS

B.1 SMS SPAM: A CONTENT-MODERATION UNLEARNING TASK

We revisit the UCI SMS Spam Collection (Almeida et al., 2011), treating the *spam* class (p_1) as information to forget and the *ham* class (p_2) as information to preserve. Messages are vectorised with TF-IDF features. Deletion budgets again span 5% to 100% of the spam slice in 5-point increments. We compare the same five scoring rules as before (COS-MU2, LR-COS, KNN-RATIO, TFIDF-NORM,

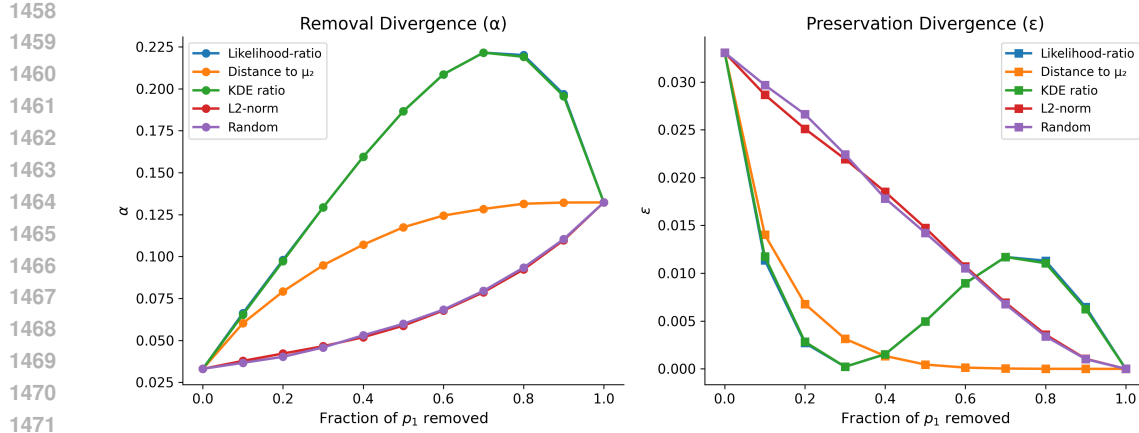


Figure 6: **Synthetic Gaussians.** Comparison of all strategies considered in the real-world datasets, using the low-divergence scenario of synthetic Gaussians (left plot, Fig. 2). Likelihood-ratio surpasses the distance-based strategy for lower deletion budgets. However, for larger budgets, it sacrifices utility for excessive removal. This is likely because it deletes samples representative of p_1 but close to p_2 since p_1 and p_2 are similar here.

RANDOM) and average results over ten random seeds. Metrics reported are *recall* on p_1 and macro-*F1* on p_2 .

Findings. We report our main findings on our SMS Spam task in Figure 5. We observe that spam recall decays gradually until 75–80% deletion, after which all methods converge to zero as p_1 vanishes. LR-COS consistently dominates: it reaches a recall of 0.60 at the 70% deletion budget, whereas random deletion does not cross that threshold until 90% deletion. Throughout, ham macro-*F1* increases slightly (see Fig. 5b), an artefact of class-imbalance—removing spam reduces false positives in the ham slice—yet the difference across methods never exceeds 0.002. These results strengthen the evidence that selective deletion offers a 1.3–1.5× sample-efficiency gain over random removal while preserving downstream utility almost perfectly.

Remark 11 (Sample vs. Computational Efficiency in Unlearning). *The computational cost of sample-level unlearning typically scales with the size of the forget set. For instance, influence-function-based approaches, such as the one proposed by Guo et al. (2020), require computing gradients and Hessian-vector products for forget samples to approximate a second-order update. Other methods, like SalUn (Fan et al., 2024), identify and modify salient model parameters by backpropagating through the network for each forget sample. Reducing the size of the forget set implies less gradient computations and hence time savings. This forget size scaling observation also holds for the large class certified unlearning methods based on noise addition (Chourasia & Shah, 2023; Allouah et al., 2025; Waerebeke et al., 2025).*

B.2 EXPERIMENTAL DETAILS

B.2.1 HEURISTIC DELETION STRATEGIES

Across all datasets, we evaluate five scoring strategies for ranking samples in the forget distribution p_1 for removal. These scores approximate statistical dissimilarity from the retained distribution p_2 and correspond to different operational interpretations of divergence:

- **LR-COS / LR-MAHA** (likelihood-ratio inspired): A proxy for the log-likelihood ratio of x under p_2 versus p_1 :

$$s(x) = d(x, \mu_2) - d(x, \mu_1)$$

where $d(\cdot, \mu)$ denotes cosine distance in TF-IDF space (text) or Mahalanobis distance in CNN feature space (images). Points are scored high when they are far from p_2 and close to p_1 .

1512 • **COS-MU2 / MAHA-MU2** (dissimilarity to p_2): Measures the distance from each $x \in p_1$ to
 1513 the empirical mean of p_2 :

$$s(x) = d(x, \mu_2)$$

1514 This approximates the contribution of each point to the KL divergence $KL(p_2 \parallel \hat{p})$ when p
 1515 is modeled as a Gaussian.

1516 • **KNN-RATIO** (local density ratio): Estimates the ratio of k -NN densities:

$$s(x) = \frac{\hat{p}_1(x)}{\hat{p}_2(x)}$$

1517 where $\hat{p}_i(x) = \exp(-\|x - \text{NN}_k^{(i)}(x)\|^2 / \sigma^2)$ is a local Gaussian kernel density using $k = 10$
 1518 nearest neighbors. This captures how typical x is under p_1 versus p_2 .

1519 • **TFIDF-NORM / L2-NORM**: Uses the ℓ_2 norm of the raw input (TF-IDF or real-valued) as
 1520 a proxy for informativeness or deviation from the origin:

$$s(x) = \|x\|_2$$

1521 • **CORESET** (centroid-based): Selects samples closest to the centroid of the forget set p_1 :

$$s(x) = \|x - \mu_1\|_2,$$

1522 where μ_1 is the empirical mean of p_1 . This strategy prioritizes representative samples that
 1523 are central to the forget distribution, potentially capturing the most characteristic patterns.

1524 • **K-CENTER** (k-center greedy): Greedy selection to maximize minimum distance coverage
 1525 of the forget set:

$$s(x) = \max_{i \in S} \|x - x_i\|_2,$$

1526 where S is the set of already selected points. This strategy iteratively selects points that
 1527 maximize the minimum distance to previously selected points, ensuring diverse coverage
 1528 of the forget distribution.

1529 • **RANDOM**: Samples points uniformly at random from p_1 as a baseline.

1530 The first two sets of heuristics are direct extensions of our Gaussian selective removal method. When
 1531 reporting results under “Selective removal” in tables, we report the best-performing heuristic among
 1532 these.

1533 **Remark 12** (Computational complexity of selection). *The selection methods evaluated present a
 1534 spectrum of computational complexities, which is a key practical consideration for their use. At
 1535 the most efficient end, methods like Random Removal, L2-Norm scoring, and the centroid-based
 1536 Coreset are computationally inexpensive. Their complexity scales roughly linearly with the number
 1537 of forget samples (n_1) and feature dimensions (d), making their cost approximately $O(n_1 d)$ plus
 1538 sorting time. Our primary selective algorithms, based on distance to the retained set’s mean, are
 1539 moderately more complex. The Cosine distance variant remains efficient at $O((n_1 + n_2)d)$, but
 1540 the Mahalanobis distance version is more demanding. Its need to compute an inverse covariance
 1541 matrix introduces a term that scales with the cube of the dimensions ($O(d^3)$), making it potentially
 1542 prohibitive for high-dimensional data.*

1543 *On the other hand, some heuristics are computationally intensive. The KNN-RATIO method is par-
 1544 ticularly costly because it requires performing a k -nearest neighbor search for every sample in the
 1545 forget set, which scales poorly with large datasets. Similarly, the iterative nature of the K-CENTER
 1546 greedy algorithm makes it much slower than single-pass scoring approaches. This highlights a
 1547 fundamental trade-off: while more complex methods like KNN-RATIO aim to capture nuanced dis-
 1548 tributional information, their computational overhead might be impractical. Simpler, faster methods
 1549 like calculating the distance to the retained mean often provide a strong, practical balance between
 1550 the effectiveness of the selection and its computational feasibility.*

1551 B.2.2 TABLE 5: SAMPLE-LEVEL UNLEARNING METHODS

1552 We evaluate five sample-level unlearning strategies that represent different approaches to machine
 1553 unlearning:

1566 • **RETRAINING** (oracle baseline):
 1567
 1568 – **Description:** Complete retraining from scratch on the retained data only. It trains a
 1569 new model from random initialization using only samples from p_2 . It provides the
 1570 theoretical upper bound for sample-level unlearning performance, representing the
 1571 gold standard but with highest computational cost.
 1572 – **Hyperparameters:** Adam optimizer, learning rate 1×10^{-3} , 10 epochs, batch size
 1573 128.

1574 • **FINE-TUNING** (naive baseline):
 1575
 1576 – **Description:** Continues training the pre-trained model on retained data only. We
 1577 initialize with pre-trained weights, then train for additional epochs on non-removed
 1578 samples.
 1579 – **Hyperparameters:** Adam optimizer, learning rate 5×10^{-4} , 2 epochs, batch size 128.

1580 • **SALUN** (saliency-based unlearning (Fan et al., 2024)):
 1581
 1582 – **Description:** This method resets parameters with highest saliency for forget samples,
 1583 then finetunes on retained data: (1) Compute saliency scores for forget samples, (2)
 1584 Reset top- $k\%$ most salient parameters to initial values, (3) Finetune on retained data.
 1585 It leverages parameter importance to selectively reset the most forget-relevant param-
 1586 eters while preserving general knowledge.
 1587 – **Hyperparameters:** Adam optimizer, learning rate 5×10^{-4} , 3 epochs, batch size 128,
 1588 topk_percent=0.2.

1589 • **NEGGRAD+** (stochastic gradient descent ascent (Kurmanji et al., 2024)):
 1590
 1591 – **Description:** This method simultaneously maximizes loss on forget samples while
 1592 minimizing loss on retained samples with loss $\beta \times \text{retain_loss} + (1 - \beta) \times \text{forget_loss}$.
 1593 This is essentially SGDA to balance retention of p_2 knowledge against forgetting of
 1594 p_1 samples through opposing gradient directions.
 1595 – **Hyperparameters:** SGD optimizer, learning rate 1×10^{-3} , momentum 0.99, weight
 1596 decay 0.1, 3 epochs, $\beta = 0.9$, batch size 128.

1597 • **INFLUENCE FUNC.** (influence function-based approximation):
 1598
 1599 – **Description:** Approximates the effect of removing forget samples using influence
 1600 functions, then applies parameter updates without retraining: (1) Compute influence
 1601 scores for forget samples using Hessian-vector products, (2) Apply parameter updates
 1602 based on influence estimates. This is computationally expensive for larger models, so
 1603 we only use it for the Gaussian experiment.
 1604 – **Hyperparameters:** Adam optimizer, learning rate 1×10^{-4} , 2 epochs, batch size 128,
 1605 damping factor 0.01.

1606 B.2.3 SYNTHETIC GAUSSIANS

1607
 1608 We draw $n_1 = n_2 = 1,000$ samples from $p_1 = \mathcal{N}(0, 1)$ and $p_2 = \mathcal{N}(\mu_2, 1)$ for $\mu_2 \in \{0.5, 2.5, 5.0\}$,
 1609 with 20 seeds. After computing scores using each strategy, we remove the top- f fraction of p_1 points,
 1610 fit a Gaussian $\mathcal{N}(\hat{\mu}, 1)$ to the retained data, and compute:

$$1611 \quad \alpha = \text{KL}(p_1 \parallel \hat{p}), \quad \varepsilon = \text{KL}(p_2 \parallel \hat{p})$$

1612
 1613 These metrics match the forward-KL objectives of removal and preservation. No predictive model
 1614 is trained; results reflect pure distributional divergence. For completeness, in Figure 6, we plot a
 1615 comparison of all strategies considered in the real-world datasets, using the low-divergence scenario
 1616 of synthetic Gaussians (left plot, Fig. 2). Likelihood-ratio surpasses the distance-based strategy for
 1617 lower deletion budgets. However, for larger budgets, it sacrifices utility for excessive removal. This
 1618 is likely because it deletes samples representative of p_1 but close to p_2 since p_1 and p_2 are similar
 1619 here. This indicates that no removal strategy strictly dominates all others across all divergence
 (between p_1 and p_2) scenarios.

1620 B.2.4 JIGSAW TOXIC COMMENTS
16211622 We use the Jigsaw Toxic Comment Classification dataset, with 140K examples filtered to length
1623 5–200 tokens. We define p_1 as all training comments containing any of the keywords: “f*ck”,
1624 “s*it”, “d*mn”, “b*tch”, “a*s”, and p_2 as the remaining comments. For each of 5 random seeds,
1625 we:1626 1. Stratified-split p_1, p_2 into 70/30 train/val.
1627 2. Compute TF-IDF embeddings (40K max features, 1–2 grams, sublinear TF, min_df=5).
1628 3. Score and remove f of p_1 training points using each heuristic.
1629 4. Downsample p_2 to 5x the remaining p_1 size.
1630 5. Train an ℓ_2 -regularized logistic regression on the edited data.
1631 6. Evaluate $Recall@p_1$ and $F1@p_2$ on the validation sets.
1632
16331634 B.2.5 SMS SPAM COLLECTION
1635

1636 We use the UCI SMS Spam dataset (5574 examples, 13.4% spam). We apply:

1637 1. TF-IDF vectorization (20K features, 1–2 grams, stopword removal).
1638 2. Scoring of spam (p_1) messages using each heuristic.
1639 3. Removal of top- f fraction of spam for each strategy.
1640 4. Retrain a logistic regression classifier.
1641 5. Evaluate $Recall@spam$ and $F1@ham$ on a held-out 20% test split.
1642
16431644 We run 10 seeds and report mean \pm standard error.
16451646 B.2.6 CIFAR-10 CLASS REMOVAL
16471648 We treat the “cat” class as p_1 and the other 9 classes as p_2 . We use the standard CIFAR-10 split
1649 (50K train, 10K test), and proceed as follows:1650 1. Train a 3-block CNN (Conv–BN–ReLU $\times 2$ + MaxPool, widths 32–64–128, global avg pool
1651 + linear head) for 10 epochs on the full training set.
1652 2. Extract features for all training images using the penultimate layer.
1653 3. Compute Mahalanobis distance scores for each cat image (p_1) using:

1654
$$s_{\text{maha}}(x) = \sqrt{(x - \mu)^\top \Sigma^{-1} (x - \mu)}$$

1655 where μ and Σ are estimated from p_2 .
16561657 4. Delete the top- f fraction of cat images under each scoring method.
1658 5. Retrain the same CNN architecture on the edited training set.
1659 6. Evaluate:

1660
$$\text{Accuracy}_{\text{cat}}, \quad \text{Accuracy}_{\text{non-cat}}$$

1661 on the test set. Results are averaged over 30 random seeds.
16621663 B.2.7 COMPUTING ENVIRONMENT
16641665 All experiments were run on a HPE DL380 Gen10 equipped with two Intel(R) Xeon(R) Platinum
1666 8358P CPUs running at 2.60GHz, 128 GB of RAM, a 740 GB SSD, and two NVIDIA A10 GPUs.
1667 Training for vision experiments was implemented in PyTorch, while text-based experiments used
1668 Scikit-learn. All experiments were conducted using a single GPU.
1669

1674 **B.3 ABLATION: SENSITIVITY TO FEATURE REPRESENTATIONS**
16751676 To assess how sensitive our selective deletion procedure is to the choice of feature representation,
1677 we conducted an ablation study on CIFAR-10 where we varied only the feature extractor and kept
1678 the selection algorithm and training setup fixed. We compare five representations: the default CNN
1679 features used in the main paper, ResNet-18 features (both pretrained and trained from scratch), and
1680 raw pixel features. For each setting, we measure forget-set accuracy at a deletion budget of 60%
1681 (lower is better forgetting). The results are shown in Table 6.1682 Two main observations emerge. First, across standard learned representations (CNN, ResNet-
1683 18 scratch, ResNet-18 pretrained), the forgetting performance is very similar, suggesting that the
1684 method is robust once the feature extractor provides a reasonably expressive embedding space. Sec-
1685 ond, using raw pixels significantly weakens forgetting, confirming that feature quality matters, but
1686 not in a way that makes the method brittle to the specific backbone.

| 1688 Feature Extractor | 1689 Forget Set Accuracy (%) |
|---------------------------------------|-------------------------------------|
| 1689 Random (baseline) | 1690 40.5 ± 2.5 |
| 1690 CNN (default) | 1691 21.6 ± 1.9 |
| 1691 ResNet-18 (trained from scratch) | 1692 20.4 ± 2.1 |
| 1692 ResNet-18 (pretrained) | 1693 27.3 ± 1.8 |
| 1693 Raw pixels | 31.8 ± 2.0 |

1694 Table 6: Forget set accuracy (mean \pm s.e.m.) at 60% deletion for different feature extractors on
1695 CIFAR-10. Lower is better forgetting.1698 **B.4 ADDITIONAL CORESET BASELINES ON CIFAR-10**
16991700 To further investigate the behavior of retain-agnostic coresets methods in our unlearning setting, we
1701 compared our selective removal strategy against two strong data subset selection baselines, CRAIG,
1702 GradMatch, and CCS, on CIFAR-10. All methods operate at a fixed deletion budget of 60% from
1703 the forget class, and we report the resulting forget-set accuracy (lower is better forgetting). While
1704 CRAIG and GradMatch slightly, though not significantly, improve over random deletion, they still
1705 operate purely on the forget distribution and cannot exploit contrast with the retain distribution. As
1706 shown in Table 7, our distributional selection substantially outperforms these baselines.

| 1708 Selection Method | 1709 Forget Set Accuracy (%) |
|---|-------------------------------------|
| 1709 Random | 1710 39.2 ± 1.9 |
| 1710 CRAIG (Mirzasoleiman et al., 2020) | 1711 36.3 ± 2.7 |
| 1711 GradMatch (Killamsetty et al., 2021) | 1712 35.5 ± 4.2 |
| 1712 CCS (Zheng et al., 2023) | 1713 40.9 ± 4.1 |
| 1713 Selective (ours) | 24.5 ± 1.4 |

1714 Table 7: Forget set accuracy (mean \pm s.e.m.) on CIFAR-10 at a 60% deletion budget from the forget
1715 class. Lower values indicate stronger unlearning. Our selective removal method, which leverages the
1716 retain distribution, outperforms all strong coresset baselines (CRAIG, GradMatch, CCS) and random
1717 deletion.